

LAPPEENRANNAN TEKNILLINEN YLIOPISTO
LUT University
Electrical Engineering

Juho Terrijärvi

Isothermal real time DNA amplification instrument

Examiners: Professor Pertti Silventoinen (LUT)
D.Sc. Tommi Kärkkäinen (LUT)
Supervisor: B.Sc. Jorge Soto (Miroculus)

ABSTRACT

LAPPEENRANNAN TEKNILLINEN YLIOPISTO
LUT University
Electrical Engineering

Juho Terrijärvi

Isothermal real time DNA amplification instrument

Master's thesis

2019

47 pages, 21 figures, 5 tables and 10 appendices

Examiners: Professor Pertti Silventoinen (LUT)

D.Sc. Tommi Kärkkäinen (LUT)

Supervisor: B.Sc. Jorge Soto (Miroculus)

Keywords: Open source hardware, isothermal DNA amplification, fluorescence

The world of open source hardware has not yet made its way to the field of biotechnology. This is mainly due to high development costs of equipment as well as governmental regulations on hardware to be used in diagnostic purposes. If one can only concentrate on research use only instrumentation, one can forget the governmental regulations. In this work an open source hardware for research purposes is presented that can run LAMP (Loop Mediated Isothermal Amplification) reactions to amplify DNA with real time detection of reaction using inexpensive optics. miriam is designed to heat a 96-well plate to a desired temperature and to maintain the temperature to enable isothermal amplification conditions. There is also a top heating plate to prohibit condensation. The optical setup is realized by using 96 LEDs alongside with 96 photodiodes that are separated from each other with an emission filter used in theatrical illumination. miriam can successfully use calcein as a fluorophore to record LAMP reaction and with a slight modification also SYBR green could be utilized as a fluorophore in assays. The design documents for miriam are publicly available (<https://github.com/miroculus/Miriam>) and the production costs per piece are below 200\$.

Used abbreviations

ADC	Analog to digital converter
API	Application programming interface
BOM	Bill of material
DNA	Deoxyribonucleic acid
IDE	Integrated development environment
LAMP	Loop mediated isothermal amplification
MOSFET	Metal-oxide-semiconductor field-effect transistor
PCB	Printed circuit board
PCR	Polymerase chain reaction
PD	Photodiode
PID	Proportional Integral and Derivative
PWM	Pulse width modulation
RNA	Ribonucleic acid
rfu	Relative fluorescence unit
RGB	Red-Green-Blue
SG/BG	Signal to background -ratio
SMD	Surface mount device
qPCR	Quantitative PCR

Table of Contents

1	Introduction	6
1.1	Miroculus.....	6
1.2	miriam	7
1.3	Open source in biotech	8
2	DNA and RNA amplification technologies.....	9
2.1	Polymerase chain reaction.....	9
2.2	Loop mediated isothermal amplification	10
2.3	Instruments for qPCR amplification	10
3	Design procedure	14
3.1	Physical dimensions	14
3.2	Optics.....	15
3.2.1	Calcein emission and excitation.....	15
3.2.2	Excitation light source	15
3.2.3	Calcein light emission measurement	17
3.3	Heating	20
3.4	Control.....	21
3.4.1	Shield PCB.....	21
3.4.2	Heating control.....	22
3.4.3	LED control and sensor.....	23
3.4.4	Wireless communication.....	23
3.5	Case	24
3.6	Assembly	25
3.7	Embedded software	26
4	Results	30

4.1	Heat uniformity	30
4.1.1	Top plate.....	30
4.1.2	Assay temperature plate	31
4.2	Fluorescent detection	33
4.2.1	First revision	33
4.2.2	Second revision	35
4.2.3	Final iteration	38
4.3	Shield	38
5	Discussion.....	40
5.1	Heating	40
5.2	Optics.....	41
5.3	Control interface	42
5.4	Electronics	43
6	Conclusions	44
	References.....	45
	Attachments.....	47

1 Introduction

1.1 Miroculus

Miroculus is a biotech startup established 2014 and its goal in the beginning was to democratize cancer diagnostics based on the knowledge of different micro-RNA (ribonucleic acid) expression levels in a blood sample. This expression status of micro-RNAs would form a fingerprint that in combination with algorithm developed by Miroculus could detect the cancer the patient was suffering from. In order to make diagnostics available for all, one of the initial key drivers of Miroculus was to lower the equipment costs to run the DNA (deoxyribonucleic acid) diagnostics. This was due to the fact that instrumentation available for DNA and RNA amplification with real time detections is highly expensive.

Together with Arduino Sweden, Miroculus started to develop an open source diagnostic instrument that could provide isothermal conditions for LAMP (Loop mediated isothermal amplification) reaction to take place so that there would be optics to constantly record the amplification of fluorescence. This would remove the need for expensive qPCR (quantitative polymerase chain reaction) capable instrumentation. The device was to have Arduino's open source hardware for control and low cost optical and heating solution to enable the reaction. Arduino is an open source platform that utilizes a physical programmable microcontroller. Simplicity comes from their own developed IDE (Integrated Development Environment) that enables easy programming of C++ and a simple way to upload the program to the physical device using Arduino's own bootloader.

Design and testing team from Miroculus consisted of one person, Juho Terriärvi, with supervision from Jorge Soto (CTO). Team utilized the knowledge and expertise from Miroculus assay team in order to acquire the necessary solutions to run assays with. First the team provided Arduino with initial specifications to be used in the electrical design of the instrument. These included the necessary light spectra and few template illustrations of current instrumentation used in DNA amplification. Based on these Arduino designed the first LED and sensor PCBs (Printed Circuit Board) as well as the first shield and template heating PCBs. Arduino also wrote the initial firmware that is the basis of all the following versions of different firmware. The prototype was assembled in a wooden box. Miroculus team aided in the design over skype and visited Malmö two times. After release of the prototype, Miroculus design team did all the iterations of PCBs, firmware and testing to release miriam.

1.2 miriam

miriam is the result of collaboration between Arduino and Miroculus. It is an open source platform for DNA or RNA amplification in isothermal conditions. miriam enables the real time detection of the amplification reaction based on the fluorescence of fluorophore calcein that becomes fluorescent during the presence of manganese ions released during DNA amplification. Most of all miriam is an open source instrument and the details how to assemble miriam are available freely online (Hence forth cited as: design document repository, <https://github.com/miroculus/Miriam>; design documents attached also to this thesis). The production costs of miriam are below 200\$, which enables the use of the equipment in low resource settings and in starting laboratories. (Figure 1.) The motivation behind miriam was to democratize DNA based diagnostics. miriam can easily be used in low resource setting with only power cord connected to device as communication can be realized either with a USB connection or wirelessly via WIFI.



Figure 1 miriam fully assembled and ready to be used in DNA or RNA amplification assays.

miriam contains 96 LEDs in combination with 96 PDs (photodiodes) that are used to detect the fluorescence from the reaction. The optics contain no additional optical components besides the LED and PD. A light emission filter can be used to enhance the fluorescence signal separation from background. This is a very inexpensive way to realize optics and one of the key reasons in the low price behind miriam.

The physical dimensions of miriam are only 275x132x75 mm. The small size is due to small scale optics and the lack of temperature cycling components. The assay technology Miroculus uses is LAMP which only requires isothermal conditions to multiply DNA. Because temperature is easy to generate and to maintain,

in miriam the heating is realized with trace heating. miriam contains two heating PCBs which are nothing but a long, narrow copper trace containing elements. The resistance of these elements is between 6 to 9 Ω and due to 12 V led through them, they generate sufficient heating conditions.

The tool used in electrical design was Eagle 7.3.0 Standard edition. What is good in Eagle, when considering open source community, is that Eagle allows the design of 100x80 mm PCBs free of charge using the Eagle free version. The PCBs used in miriam are 142.5x97.5 mm so they are a bit wider and longer than allowed by the free version of Eagle. But free version allows to open, view and to modify the PCBs by their components in the 100x80 mm area. Free version also allows to draw traces beyond the free area. All the components in miriam are located in 100x80 mm area and hence they can also be modified using free version of Eagle.

1.3 Open source in biotech

Open source hardware has not yet reached the field of diagnostics. This is mainly due to really high development costs of the machines used in diagnostics as well as the regulatory demands set by legislation like different directives. One of the key directives in Europe is the directive concerning In vitro diagnostic medical devices directive (IVD 1998). The directive contains steps in order to ascertain sterility of the device, quality of data provided and performance of the instruments, the instrument complying with the directive needs to be compliant to other directive compliant instruments and the device needs to be safe to operate. The development costs and costs on complying directives cause such a strain to instruments that their prices climb so high that launching them open source could never bring back the development costs.

Still there are a few who have launched open source diagnostic devices. Usually these devices are meant for research use only, because research use only equipment does not need to comply with the directives. On the down side, the results obtained, when utilizing this kind of equipment, can only be used in research purposes. One very inexpensive open source project is the OpenPCR (OpenPCR 2019). OpenPCR contains a Peltier-element that cycles the wanted temperatures on vials that are placed on the element. OpenPCR functions also with an Arduino microcontroller. The project does not contain any optics and hence the price is only 499\$. Another example is an open source qPCR machine from Chai (Chai 2019). The machine supports four different fluorescent dyes and works with a 16-well plate. The fluorophore excitation window is quite small, ranging only from 454 nm to 487 nm, but the emission window is a bit wider 508-597 nm. If purchased new, the price starts from 4500\$.

2 DNA and RNA amplification technologies

2.1 Polymerase chain reaction

Polymerase chain reaction (PCR) means the amplification of nucleic acids and is sometimes called as “molecular photocopy”. It was first developed by Kary B. Mullis in the 80s and he was awarded with a Noble Prize for Chemistry in 1993 for his discovery. For the traditional, still mostly used, PCR the sample DNA is first heated so the DNA denatures, or separates into two pieces of single-stranded DNA. Next, the temperature is lowered so a polymerase, an enzyme that copies DNA strands, binds to the single-stranded DNA strands and remakes them double-stranded. Polymerase requires oligos, template beginning strands, that first bind to single-stranded DNA molecules. Once the polymerase has finished the copying, the cycle is repeated. This leads to exponential amplification of DNA. (NIH 2015.) RNA amplification by PCR based means, requires first turning RNA into DNA by the use of reverse transcription enzyme. The enzyme produces a complementary single-stranded DNA strand called cDNA from single stranded RNA molecule. This single stranded cDNA can then be used as a template in above described PCR reaction. (ScienceDirect 2017.) PCR can be used in all applications requiring the multiplication of DNA or RNA. Some of these can be detection of genetic disorders (Boehm 1989), viral and bacterial contaminations (Tuladhar et al. 2012) etc.

In the beginning PCR was used to amplify the DNA to seek and then the recognition of the possible amplification product was qualitatively done by staining the possibly amplified DNA with a colorful stain. The problem with this method was that the amplification of low amounts of DNA takes time. One single cycle can take around one minute and usually 60 cycles are required to fully reach total amplification level. Then the staining was yet another step in the process taking time. Hence multiple quantitative approaches were developed quite early that have revolutionized the 21st century biological science. These qPCR methods normally utilize fluorescence so that during the amplification of DNA the fluorophores in the reaction become increasingly active when they bind double stranded DNA or by combining with released metal ions during the reaction (Deepak et al. 2007, Liu et al. 2017). Calcein is an example of a dye that becomes fluorescent because binding to manganese ions. These qPCR-based methods quicken up the detection of positive and negative reactions and they also enable calculating the original amount of DNA strands.

There are as many qPCR detection methods as there are manufacturers of the equipment to be used in qPCR. Most of the solutions still use light as the means for detection. There can be a CCD or CMOS camera

taking a picture of the reaction plate and then the reaction can be detected by calculating the light intensity of fluorescence from certain pixels of the image. The light detection can happen with a mechanically circulating PD (photodiode) or avalanche PD that measures the light intensity one sample at a time or there can be a photomultiplier tube doing the reading. There are some approaches that use electronic microarrays as a detection mechanism of PCR reaction but these are mainly just raising technologies (Thanthrige-Don et al. 2018).

2.2 Loop mediated isothermal amplification

Loop mediated isothermal amplification is a nucleic acid amplification technology quite like PCR. The main difference between these two is that PCR requires temperature cycling as LAMP happens in isothermal conditions, usually between 50-65°C. LAMP was first released in the beginning of 2000 (Notomi et al. 2000). In LAMP the DNA strands contain so many similar regions that recognize each other so that when they become single stranded, they anneal so that multiple single stranded loops are formed. These free, single stranded loops, can bind the DNA or RNA strands to multiply and they serve as the primers for the amplification enzyme also used in PCR. The polymerase has an ability to displace double stranded DNA and keep on amplifying product as long as there is a supply of free nucleotides.

The greatest benefit of LAMP is that the reaction happens in isothermal conditions. Hence less sophisticated device is required to enable suitable conditions for the reaction to occur. If real time detection of reaction is wanted, similar kind of optics are still required as in qPCR equipment and hence most of research teams utilize same bulky equipment in LAMP as in qPCR. One hindrance in LAMP is that it does not so easily enable exact quantification of the original DNA as qPCR does. In PCR calculating the original DNA quantity is easy because the DNA is amplified exponentially as in LAMP the reaction is not cycle based. LAMP can still serve easily as a fast and simple qualitative tool for DNA amplification-based diagnostics.

2.3 Instruments for qPCR amplification

qPCR instruments, because of thermal cycling and very sensitive optics, can be really expensive. High cost optics are required to enable sensitive detection of first occurrences of predefined signal-to-background (SG/BG) fluorescence level once the reaction starts to happen. This first occurrence of fluorescence can be compared to a standard run alongside the unknown samples and the initial quantity of sample can be calculated. Thermal cycling is a strain because the instrument needs to get rid of the excess heat produced and this increases the equipment dimensions. What increases the costs, besides optics, are the

governmental requirements for the instrumentation that the research teams can rely on. The markets for qPCR instrumentation are concentrated to few main companies. In Table 1 is gathered few of the main companies producing qPCR instruments and the instrument prices. The availability of new instrument prices is hard, because they tend to be quote only offers directly to customers and hence the table is populated with used instruments.

Table 1 qPCR instrument manufacturing companies and instrument prices taken from ebay (read 20.4.2019).

Company	Instrument	Detection method	Condition	Price \$
BioRad	iQ5	CCD camera	used	5745
Applied biosystems	ABI7500	CCD camera	used	12999
Qiagen	GENE6000	Photomultiplier	used	9999
Agilent	Mx3005	Photomultiplier	used	7999

All the equipment function with quite similar principle. All the manufacturers have their own way of designing the equipment, but mainly they are comprised of few identical features. The assay plate is usually heated and cooled with a Peltier-element controlled metal block that creates the case for the assay plate. The exciting light is usually an LED or a halogen lamp. Halogen lamp is usually used with a slightly higher price instruments that are capable of handling multiple different fluorophores due to white light the lamp generates. The white light can then be filtered to appropriate wavelengths. LED provides slightly cheaper solution, but multiple LEDs are needed in order to support multiple detection technologies. Light detection happens usually via photomultiplier tube, CCD or photodiode, lenses to collect the light, filters to filter the light and mirrors.

Usually the reaction plate is sunk into the heating element and the excitation and detection happen from above the plate. In between the optics and the assay plate is usually a window, made of indium tin oxide to properly isolate the dirty reaction from clean optics. In Figure 2 is represented an example from BioRad iQ5 real time PCR detection system optics. In the figure is represented how the light source is a Tungsten halogen lamp that provides high power and quite homogenous, e.g. white, light spectra. Right after the light source, to select the appropriate wavelength for the optical dye, is an excitation filter wheel. The iQ5 platform is capable to excite fluorophores with six different wavelengths. With mirrors the light is guided evenly to the assay well plate. The emission light from the assay wells is collected with a lens array above the well plate guided with a mirror to emission filter wheel. Emission filter wheel, when used in

combination with the excitation filter wheel, makes it possible to distinguish six different fluorescent channels. A CCD camera takes a picture of the collected light and from the pixels of the image, image calculation algorithm can be used to plot the intensities per sample well.

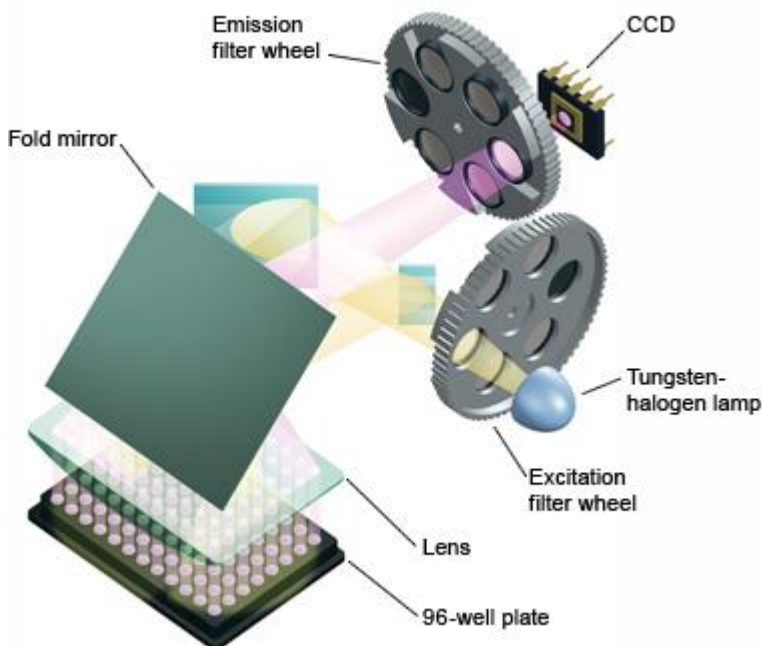


Figure 2 BioRad iQ5 real-time PCR detection system optics (BioRad 2019).

Usually heat is generated with a Peltier-element because the PCR reaction requires fast cycling between low and fast temperatures. Figure 3 explains the cycled temperatures in PCR that range from almost 100°C to as low as 40°C. Faster the temperature change can be done, faster the whole assay can be performed. The temperatures used in the figure are only reference temperatures because each manufacturer of PCR reagents have their own protocol to follow in the reaction.

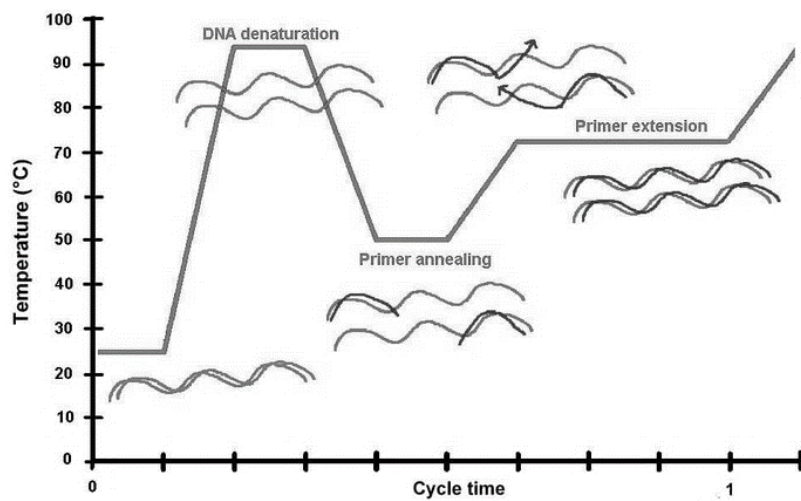


Figure 3 One PCR cycle explained and reference temperatures in the cycle.
(https://www.mun.ca/biology/scarr/PCR_simplified.html)

Besides Peltier-elements, there are few alternative ways to create looping temperatures, but they are less used. These alternatives could be i.e. keeping required amount of constantly same temperature heated elements and robotically moving the reaction plate between these heated elements (Abacus Diagnostica 2019).

3 Design procedure

3.1 Physical dimensions

miriam's dimensions originate from 96-well plate that has established its position in the field of biotechnology as a standard assay platform. 96-well plates are available in all colors as well as transparent and miriam was designed for the transparent plates. There is no consistent plate dimension standard and all the manufacturers have slightly different plate dimensions. In Figure 4 is presented the 96-well plate from BioRad miriam was designed to run assays with. Because the plate is 128x85 mm in area it was possible to dimension miriam to 275x132 mm still so that the plate occupies 30% of the whole area of the instrument.

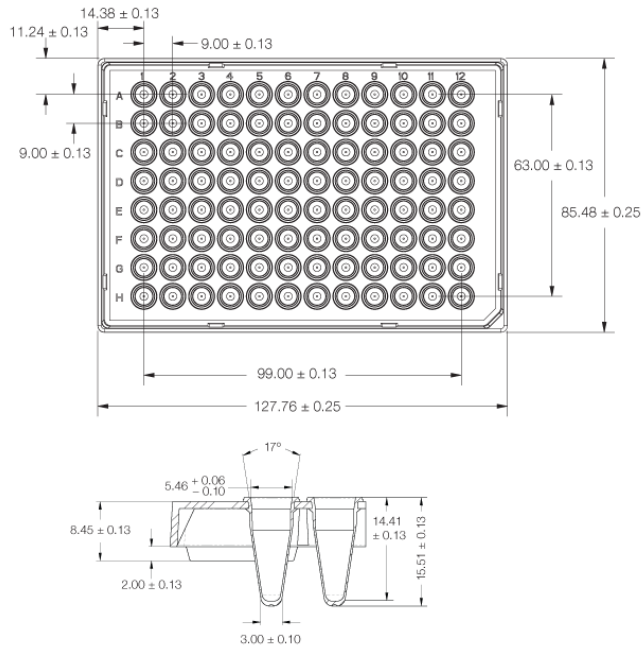


Figure 4 96-well plate from BioRad that miriam was designed to house.

In biotechnical assays, the sample is pipetted to wells of the assay plate, usually the volume is 10 to 20 μ l, and the well plate is sealed with a tape to stop the possible condensation from evaporating and to avoid spillage.

3.2 Optics

3.2.1 Calcein emission and excitation

Fluorophores are substances that excite with certain wavelength of light. One of their electrons jump to a higher orbit. When this excited electron returns to base orbit the fluorophore emits a photon. The photon that excites the fluorophore has more energy, lower wavelength, than the emitted photon. The energy lost is transformed to heat and the wavelength shift between the exciting photon end emitted photon is called Stokes shift.

The fluorophore Miroculus uses is called calcein. Calcein becomes fluorescent with a presence of manganese ions that are released during DNA amplification reaction. Calcein's excitation happens with blue light and the emission happens mainly in the green region of spectrum (Figure 5). The Stokes shift for calcein is 24 nm.

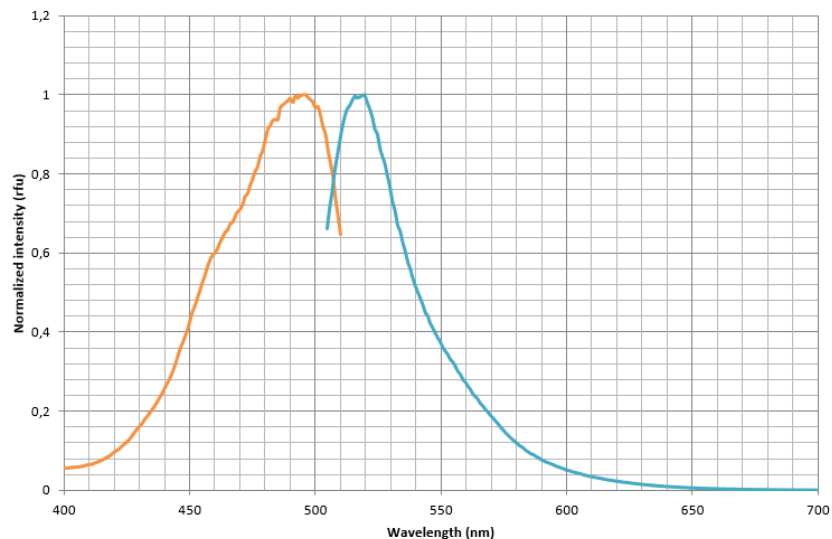


Figure 5 Calcein emission and excitation spectra. Orange: Excitation with peak wavelength 496 nm; Blue: Emission with peak wavelength 520 nm.

The excitation spectrum of calcein has a shoulder around 460 nm which is quite beneficial because there is a wide selection of LEDs at 460 nm. The emission spectrum is quite wide, but the emission intensity degrades quite fast and at 550 nm remains only 38% of the emission peak intensity.

3.2.2 Excitation light source

The problem with designing optics is that the exciting light must not penetrate to the measurement channel. Easiest option to achieve this is to use light filters that remove the light with unwanted

wavelengths and allow only light with wanted to penetrate. The problem with light filters is especially their high cost as well as the filter physical dimensions. The light filters require collection of light via lenses and light paths to be designed that require space. Due to these constraints, Miroculus wanted to avoid using light filters in miriam.

Another easy way to remove the problem of light leaking from excitation to emission channel is to use the width of the excitation spectrum alongside with Stokes shift. If the LED is selected with lower peak wavelength than the fluorophore excitation maximum, less light will leak to emission channel. The problem with this approach is that the excitation efficiency decreases rapidly with changing the exciting light peak wavelength. This loss can be compensated with increased light intensity. The increased light intensity on the other hand causes harm because of photobleaching phenomenon. Photobleaching is the destruction of fluorophores due to constant excitation (Gordon et al. 2004).

Another way to prohibit the unwanted light leakage is to mount the components so, that the light channels from excitation and emission do not cross paths. In miriam this approach has been utilized. Usually the easiest optical alignment is to place the light measurement directly after the sample in the same optical channel where the excitation comes from. Luckily the availability of angle mount SMDs is abundant and in miriam two different angle mount SMDs were tested. Both LEDs were from Kingbright and the main difference between the LEDs was the physical size of the component. Properties for both of the LEDs can be seen in the Table 2.

Table 2 The main data of LEDs selected.

	AA4040QBS/D	KA-2810AQBS-G
Manufacturer	Kingbright	Kingbright
Dimensions	4.0x3.6x4.0 mm	2.8x1.2x0.8 mm
Peak wavelength	460 nm	461 nm
Dominant wavelength	465 nm	465 nm
Spectral half-width	25 nm	25 nm
Forward voltage	3.3 V	3.3 V
DC forward current	30 mA	30 mA

Calcein excitation peak wavelength is 496 nm and both of the LEDs peak wavelength are quite close to this, on the calcein excitation spectrum shoulder. The half-width of spectral lines is also 25 nm meaning

that the light intensity pattern is really narrow and the intensity is halved before 473.5 nm, lowering the probability of light from LED being interpreted as light from fluorophore. (Figure 6.)

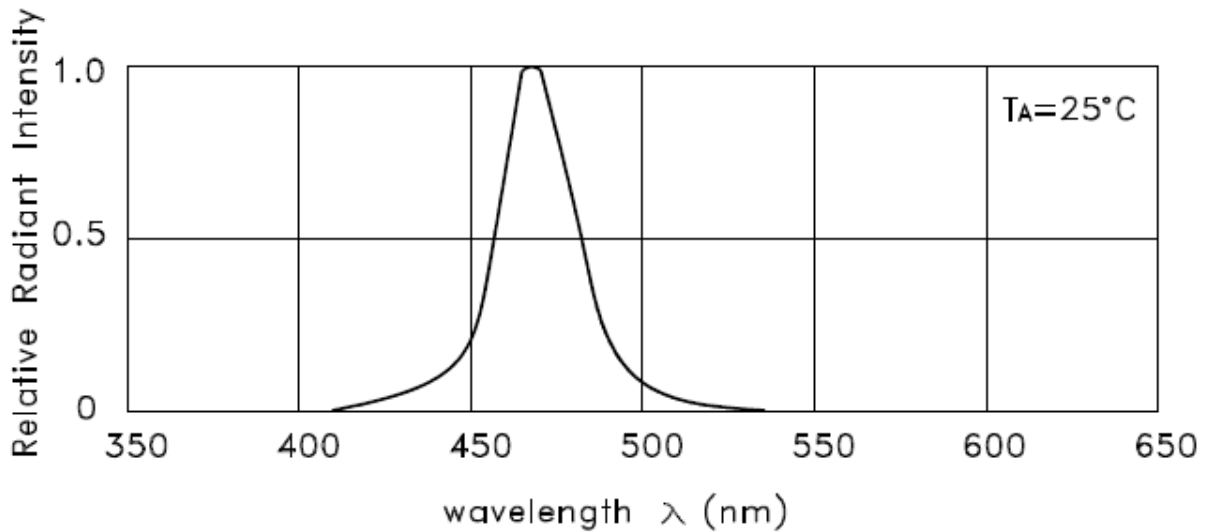


Figure 6 Led wavelength spectrum with peak of 461 nm (Kingbright KA-2810AQBS-G).

The forward voltage for the LEDs is 3.3 V and the DC forward current 30 mA. The PCB housing the LEDs was designed so that there are three LEDs in series with a resistor. The minimum required resistance for the resistor can be calculated with

$$R = \frac{V_s - n_{led} * V_f}{I_{FC}}$$

, where V_s is the supply current (in case of miriam 12 V), n_{led} the number of LEDs in series, V_f the LED forward voltage and I_{FC} LED forward current. The highest light intensity can hence be achieved with using an LED with $70\ \Omega$ resistance. To lower the number of components on the PCB resistor arrays were used with 4 resistors in one array.

The LED PCB contains 96 LEDs in 32 series of 3 LEDs and 8 pieces of 4 resistor containing arrays. The LEDs are placed next to 96 holes that allow an assay plate to pass through the holes so that the reagent volume level is above the angle mount LED.

3.2.3 Calcein light emission measurement

Fluorescence light measurement can be implemented with using either different camera-based options, using CMOS or CCD cells that can be used to record the light intensity from emission source either by

taking a picture and using picture algorithms to calculate the light intensity in certain part of the picture or directly. One way is to use photomultiplier tubes that with high voltage cause a chain reaction where the photon is first turned into an electron that bounces producing additional electrons and this electron flow can then be turned into a digital light reading. Avalanche photodiodes also utilize similar kind of a phenomenon as photomultiplier tubes where the photon striking PN junction of the diode causes a chain reaction due to voltage upheld between the PN-junction. The problem with above mentioned principles is that even though they are really sensitive, they tend to be quite expensive. The cheapest available solution, also used in miriam, is a simple photodiode.

To overcome the problem of light from excitation source leaking to fluorophore emission light measurement channel, normally light filters are used. As said, these filters tend to be quite expensive making the optics expensive. Luckily there are available a number of RGB (Red-Green-Blue) photodiodes that have their own internal filter.

In miriam two different RGB-photodiodes were tested. Both of the photodiodes had similar PCB footprint and were from the same series of Everlight RGB photodiodes. One was a green and the other a red photodiode. The sensitivity spectra for the PDs are presented in Figure 7. With the green PD the 550 nm peak emission corresponds well with calcein emission spectrum, because calcein still has 36% from the emission peak remaining at 550 nm. The green one is also quite suitable for both of the LEDs because at 465 nm the PD has spectral response of 10%. The red PD is no longer that suitable for calcein because it has only 5% of spectral response at calcein emission peak wavelength, but the red PD is better suitable for the LED spectra.

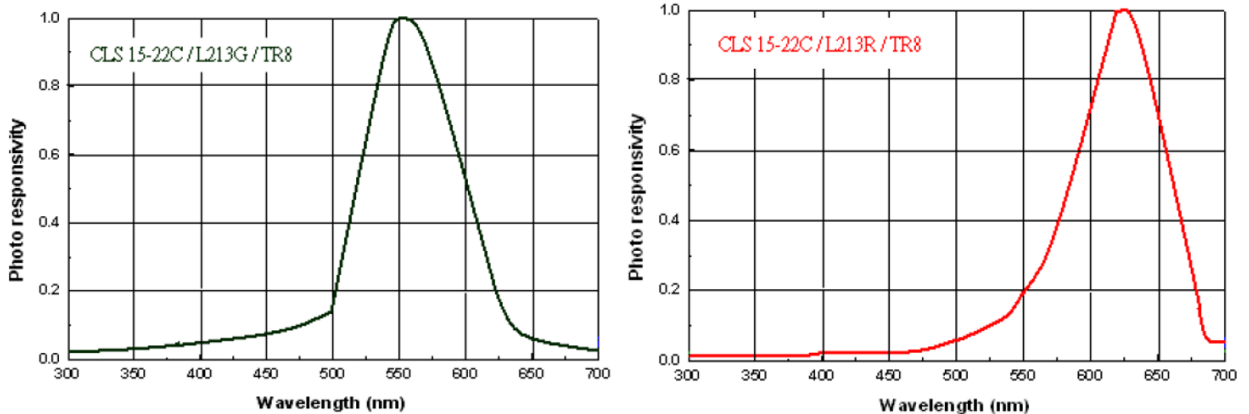


Figure 7 The two photodiodes selected for miriam. Left is the green photodiode with peak sensitivity of 550 nm and right the red photodiode with peak wavelength of 620 nm.

Photodiode is also positioned below the reaction well plate well so that the measured light path does not cross exciting light path. To be absolutely certain that no light from the LED is read by the PD also an emission filter is used to block the excitation light. The emission filter is obtained from a theatrical equipment retailer in Sweden and the filter is normally used in theatrical lighting conditions. This GAM-388 filter in the matter of fact is a really efficient notch filter (Figure 8). At 461 nm the GAM-388 allows only 1.8% light to pass the filter and at 520 nm unluckily only 5.7%. But at 550 nm the transmittance is already 65% and calcein emission intensity at this wavelength still reaches 36%. The main advantage alongside with the very efficient LED light blocking is the price of the filter. One square meter of the filter costs 10\$.

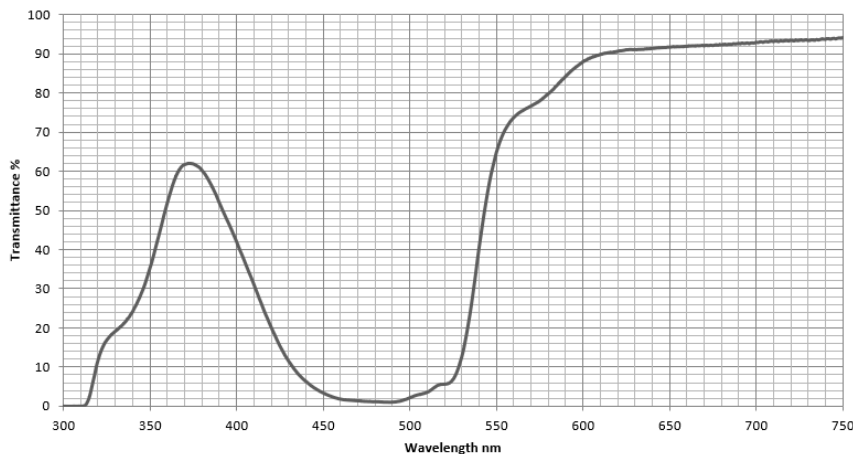


Figure 8 GAM-388 emission filter transmission spectrum.

The maximum light current for both of the PDs is only 0.72 uA and needs to be amplified drastically before the Arduino ADC (analog to digital converter) reading. This is done with a 4-channel operational amplifier arrays with each operational amplifier in the array having a 3.9 MΩ resistor in an inverting operational amplifier configuration. With this configuration the maximum light intensity can be changed from 0.72 uA to 2.8 V with equation

$$V_{out} = -I_s * R_f$$

, where V_{out} is the output voltage wanted, I_s is the light current and R_f the amplification resistor.

The outputs of operational amplifiers are connected to a 1x16 channel analog multiplexer/demultiplexer. The multiplexers are required so we can utilize Arduino Mega's internal ADC. All together there are 16 analog channels in Arduino Mega, but connecting 16 operational amplified PD signals to one multiplexer, we only need 6 ADC channels. The selection of the channel to measure happens with digital control of

selection bits of the multiplexers. All the multiplexers are controlled similarly and simultaneously, so we only need the required 4 selection channels.

The whole optical setup can be seen in Figure 9. All together there are 96 pieces of these similar kinds of setups that share the same PCBs and same emission filter.

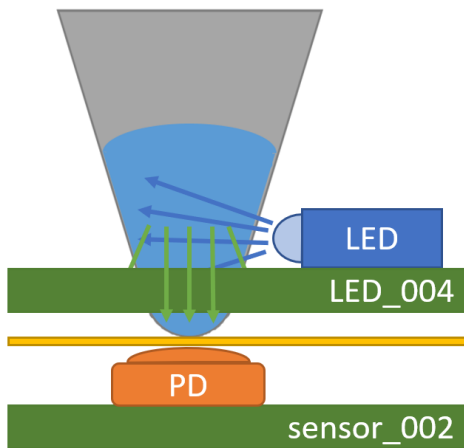


Figure 9 Schematic representation of the optical alignment used. LED is an angle mount SMD pointing towards a sample well. The fluorescent light passes the hole in the LED_004 PCB and passes an emission filter to a PD on the sensor PCB.

Different kinds of optical setups were also considered when first designing miriam. These optical setups included both the PD and LED to be angle mounted below the reaction wells. The second option was to place the LED directly on top of the assay well and directing the LED light directly through the well to a PD mounted below the bottom of the well. The setup with both components side mounted was discarded because no suitable angle mount RGB PDs were found and this would have required a mechanically designed piece to house both the PD and the LED. The concept where LED light would have been directed directly via the well was discarded because in miriam light filters were to be avoided. Also making the top heater PCB would have been quite more complicated.

With the selected setup it was possible to avoid the use of additional components besides regular PCBs. Also mounting the SMD components is easy, even automatically using PCB supplier equipment. The setup does not require any additional components besides the case housing the PCBs.

3.3 Heating

A benefit in utilizing LAMP as means for amplification is that we do not need to cycle the temperatures. We only need to keep a constant temperature of 65°C. The temperature of the reaction originates from

the chemistry used by Miroculus in their assay. In order to stop evaporate condensing to well covers, there is also a second heater in miriam that keeps constant temperature in the top of the well plate at 80-90°C.

Producing heat is easy. In miriam this is done with an N-channel MOSFET (Metal-oxide-semiconductor field-effect transistor) controlling 12 V voltage supply to very long copper traces. These traces are really narrow, only 0.254 mm in the lower heating board and 0.635 mm in the upper heating board, but they are really long. In the middle of both boards is an NTC thermistor of $10\ \Omega$ that measures the generated heat. The traces form a pattern on the PCB that has wider trace gaps on the middle than on the edges of the PCB. This is due to the fact that the temperature is measured from the middle of the PCB which is the core of the device and hence that is the place where the heat will be concentrated. The wider trace gaps are to concentrate the heat generation to the edges of the PCB.

The thermistor resistance is constantly followed connecting it to one of the Arduino Mega's ADC channels. The internal algorithm utilizes PID (Proportional integral and derivative) control with PWM (Pulse width modulation) to control the voltage with MOSFET to the heating boards. PWM is calculated every time Arduino loop-sequences is ran.

Lower heating board is aluminum 1.6 mm thick PCB. Aluminum because heat is also generated to the PCB itself, FR4 works as a heat insulator and aluminum distributes the heat more evenly. Upper heating board is FR4 to make it lighter.

The resistances of the heating boards were calculated during design phase utilizing online available trace width calculators (i.e. <https://www.4pcb.com/trace-width-calculator.html>). But already in the beginning multiple iterations of the designs were made in order to set the resistance to a desired level of few Ω s and to create even distribution of heat. The upper heating board has traces only on bottom side of the PCB and the resistance of the board is $6.2\ \Omega$. Hence the upper heating board power demand on full load is 23.2 W. The lower heating board is double sided PCB with both sides having a similar trace pattern. These sides have been connected in parallel and the resistance of the board is $8.4\ \Omega$. Hence the lower heating board power demand on full load is 17.1 W.

3.4 Control

3.4.1 Shield PCB

All the control electronics of miriam are concentrated on a shield that is to be connected directly to Arduino Mega's female 2.54 mm pitch connectors.

In this launch version of miriam an ATX computer power source is used as a power source. This was the easiest option in the initial demo version of miriam to test out the functionality of all the components and DC/DC converters due to the fact that all of these voltages were already available in the power source outputs. A computer power source can also provide hundreds of watts of power and the full load situation of miriam with both heaters heating and LEDs on simultaneously is close to 90 W. The shield has an ATX connector and in the released version, only 12 V is utilized from the ATX connector. The 12 V is fed directly to the heating boards and to LED board. Arduino Mega is also powered through 12 V from the ATX power supply. Then the return from heating boards is connected to ground plane over N-channel MOSFETs to enable PWM control. 12 V is converted to 5 V and further on to 3.3 V. The 5 V is used in thermistor resistance calculation, 3.3 V voltage regulator takes 5 V input and the WIFI module requires 3.3 V to operate.

3.4.2 Heating control

Heating control is simple and both heating boards function with a same kind of principle presented in Figure 10. In the illustrative schematic is represented how 12 V is connected directly to ground via an N-channel MOSFET. Between 12 V and ground, before the trace heater, is a glass passivated junction fast switching rectifier functioning as a diode for overvoltage protection. The trace resistance of the heater boards is few Ω s and in the middle of the trace pattern is a 10 Ω NTC thermistor. The voltage of the thermistor is read by using 5 V and voltage distribution. In Figure 10 the channel to be read, is marked with TH1. By using PID control, the temperature is read and turned into PWM output for the MOSFET.

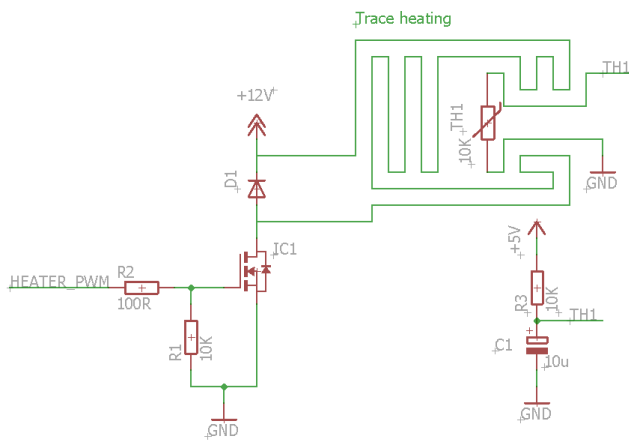


Figure 10 Heating board and control. Line HEATER_PWM is PWM output from Arduino, R2 100 Ω resistor, R1 10 Ω resistor, IC1 an N-channel MOSFET, D1 a diode, TH1 NTC 10 Ω thermistor, R3 10 Ω resistor and C1 10 uF capacitor.

MOSFET control line contains two resistors. Before gate is a resistor to stop ringing phenomenon, parasitic oscillation between the gate capacitance in series with the connecting wire's inductance. This would lead to transistor dissipating excessive power. There is also a pull-down resistor to prohibit the line to be left floating.

3.4.3 LED control and sensor

LED control follows similar kinds of principles as the heater control (Figure 11). 12 V is supplied to the LED board which has always three LEDs in series connected with one resistor array element. The LED ground is connected to ground via an N-channel MOSFET. Between 12 V and ground before the MOSFET is a diode like component as in the heater boards to shield the channel from over voltages. In the LEDCNTRL line is a $100\ \Omega$ resistor before the gate and the control line is pulled to ground with a $100\ \Omega$ resistor to stop floating control voltage.

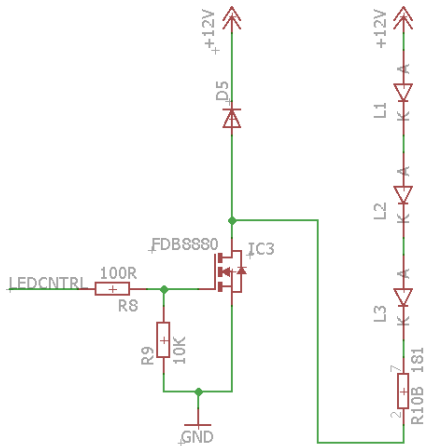


Figure 11 LED control. IC3 is an N-channel MOSFET, L1-3 LEDs, R10B 181 Ω resistor array element, LEDCNTRL a digital control line, R8 100 Ω resistor, R9 10 Ω resistor and D5 is a diode.

The shield PCB has only male connector jacks for sensor control and for analog channels from multiplexers. The control of the multiplexer's functions with four digital channels that are controlled either high or low depending on the channel to read. The configuration for the channel selection follows the multiplexer channel selection truth table (available in the design document repository).

3.4.4 Wireless communication

Two alternative ways to enable wireless communication were considered in miriam. One utilizing Bluetooth- and one WIFI-module. The Bluetooth-module was HM-10 Bluetooth 4 LTE module and the WIFI-module ESP8266. Both of these modules utilize RX/TX communication and provide a wireless way to

fulfill the protocol requirements. Both of these modules work with 3.3 V and hence there needs to be voltage distribution to 3.3 V from Arduino 5 V TX/RX lines.

Arduino Mega's second serial communication channel is connected to a one of the modules (For reference only WIFI connections are displayed in the Figure 12).

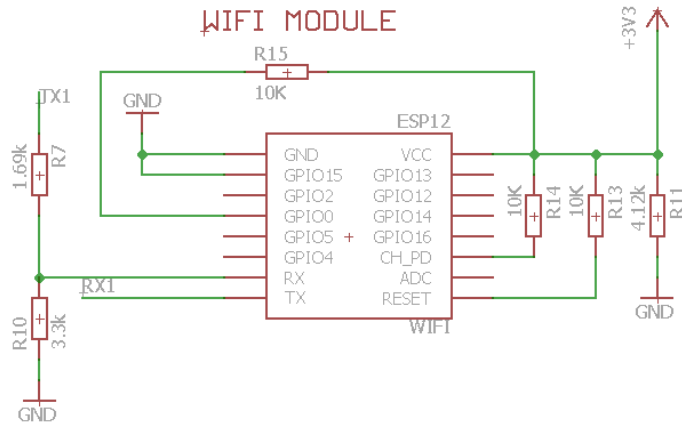


Figure 12 WIFI module schematic. TX line contains voltage distribution resistors R7 1.69 Ω and R10 3.3 Ω. Other resistors and connections can be seen from ESP design documentation.

ESP8266 is a low cost WIFI dongle from China that can translate TX/RX message to TCP/IP protocol. It works with a small built-in flash memory. Otherwise the connections follow the manufacturer specifications available in ESP Wikipedia (<https://www.esp8266.com/wiki/doku.php?id=esp8266-module-family#esp-12>).

3.5 Case

The case consists of three pieces that can be 3D-printed. The STL files to be printed out are located in the design document repository. In the design of the pieces a 0.5 mm error tolerance was used to better fit the pieces to each other. In printing appropriate layer height needs to be set to ascertain good printing quality. Suitable material for printing is i.e. PLA.

The main body houses lower heater, LED and sensor PCBs and the optical emission filter between the LED and sensor boards. On top of the section where the above-mentioned PCBs are assembled is the top cover that can be opened to insert an assay plate. The cover houses the upper heater PCB to stop the condensation. The main body also has a back compartment where the control electronics are located (shield and Arduino Mega). This back compartment can be closed with a cover. (Figure 13.)

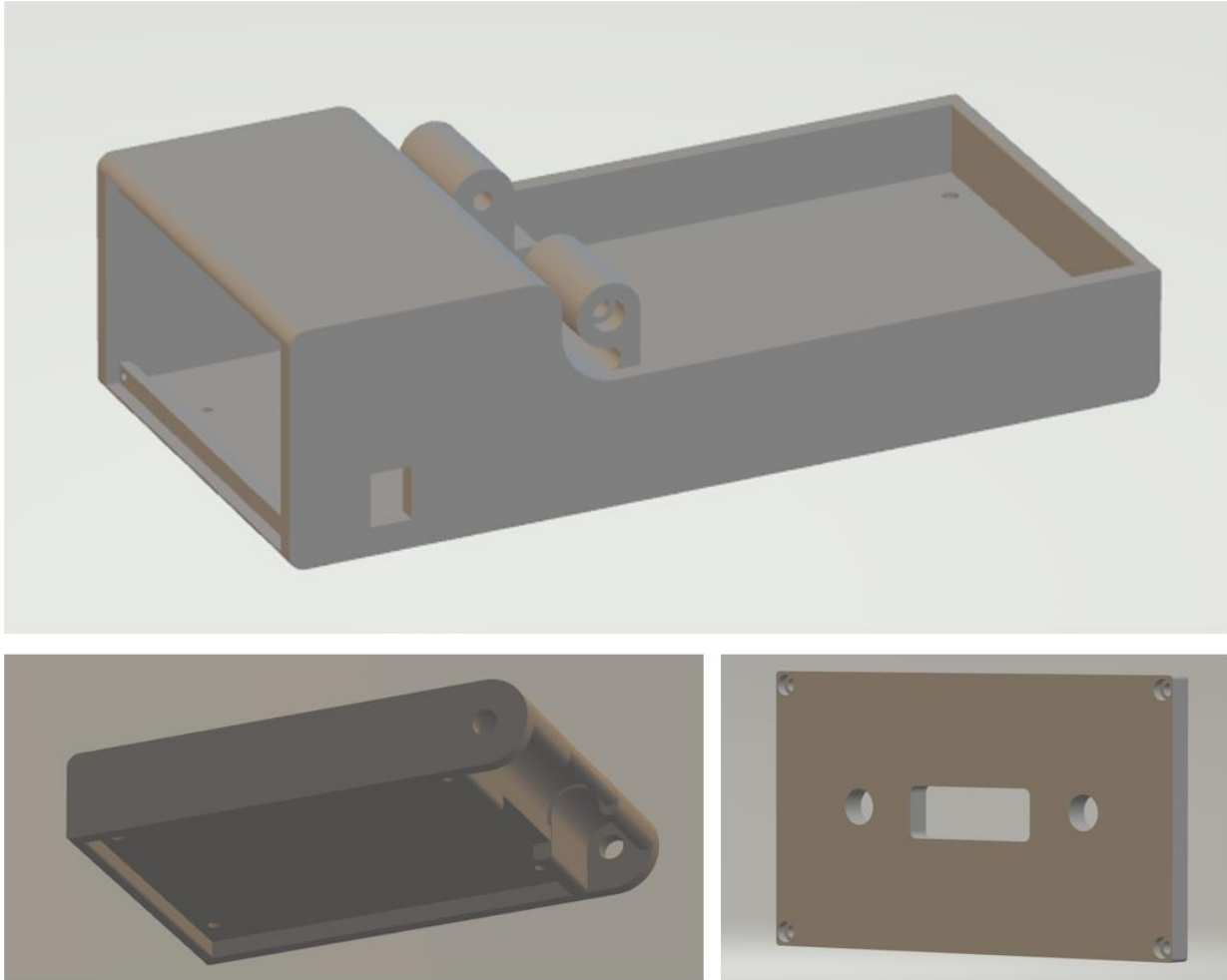


Figure 13 Three pieces that comprise the case for miriam. Upper figure is the main body that houses Arduino Mega with shield in the back and the front contains the lower heater and the LED and sensor boards. Bottom left figure is the top cover that contains the upper heater and bottom right is the back cover to hide Arduino behind it.

All the printed pieces require extensive sanding in order to align properly, especially the rounded hinge between main body and the top cover to glide smoothly. There is no suitable hole in the 3D model to power jack, if a jack is to be used. A hole suitable can be drilled next to the USB jack back of the main body.

3.6 Assembly

All the PCBs are 1.6 mm in height and they were ordered with white soldermask and black silkscreen. They were 35 um copper with gold plating. The PCB material was FR4 for all except lower heater PCB. The gerber files for the PCBs can be found in the design document repository. The gerber packages contain also mount-SMD-files to aid in automatic assembly. All the PCBs, which contain SMD components, also have Fiducial Marks to work as reference points in automatic assembly.

To assemble the PCBs to a working configuration M3 nuts, bolts and washers are needed. The bolts needed are 8 mm and 20 mm long. All the PCBs contain four holes in each corner of the PCB that are wide enough for an M3 bolt. In the upper heating board are four pieces of 8 mm bolts (see Figure 14). The 20 mm long bolts house the middle heating board, LED board and sensor board. Between middle heating and LED boards is a bit wider gap so that the LED light path will be under the 96-well plate well liquid surface.



Figure 14 PCB assembly to bolts with one of the four bolt configurations displayed, the remaining three are similar.

The bolts are placed to their holes in the main body and in the cover. They are joined to the 3D printed pieces using heat durable epoxy.

All the boards are connected to the Arduino and shield using connector cables that can be passed from the assay area to the back of the case from a hole between the body's two segments.

3.7 Embedded software

There are three different versions of embedded software for miriam available in the release version. All three share the same API (application programming interface) but have different features on how to establish communication. The interaction between miriam and the user either functions via serial communication using the USB jack of Arduino or TCP/IP messaging protocol over WIFI. The API is described in Table 3 and all the parameters to send and receive are string messages.

Table 3 API for embedded miriam software for all three versions released.

Parameter	Description	Response
'R'	Perform the fluorescent read of all the 96-wells by first measuring the dark PD signal three times and then subtracting that from average of three signals with LEDs on.	Semicolon separated array of all 96 measurements.
'i'	Return the PWM outputs to heating PBCs and the temperatures.	Semicolon separated array of PWM output, raw temperature and temperature in Celsius first for lower heated and then for upper heater.
'U XX'	Set the wanted temperature for upper heater with space separated parameter after character 'U'.	Recognized with message 'NEW UPPER TEMP: XX', where XX is the space separated parameter.
'M YY'	Set the wanted temperature for lower heater with space separated parameter after character 'M'.	Recognized with message 'NEW MIDDLE TEMP: YY', where YY is the space separated parameter.
'H'	Put the PWM output control for heaters on.	Recognize with message 'HEATING BOARDS'
'C'	Cancel heating for both heaters.	Recognize with message 'Cancel'

The easy C++ program layout of Arduino IDE makes it simple to construct a state machine where the internal state is changed with the above-mentioned parameters. Because miriam uses Arduino Mega, no modification was made to the header file that contains the port mapping required to operate the analog or digital ports of the Atmega processor.

All versions of the embedded software utilize Arduino written C++ PID control algorithm with only parameters for proportional, integral and derivative gains set in the written firmware. The parameters are changed between aggressive parameters used in the beginning of heating to conservative parameters used to upkeep the wanted temperature. Especially the derivative gain is changed drastically between the gain parameter sets. A temperature correction equation was realized to correct the read temperatures to

set temperatures for the lower heater PCB (Figure 15). The exact temperature was not that important for the top heater and hence similar kind of a correction equation was not realized.

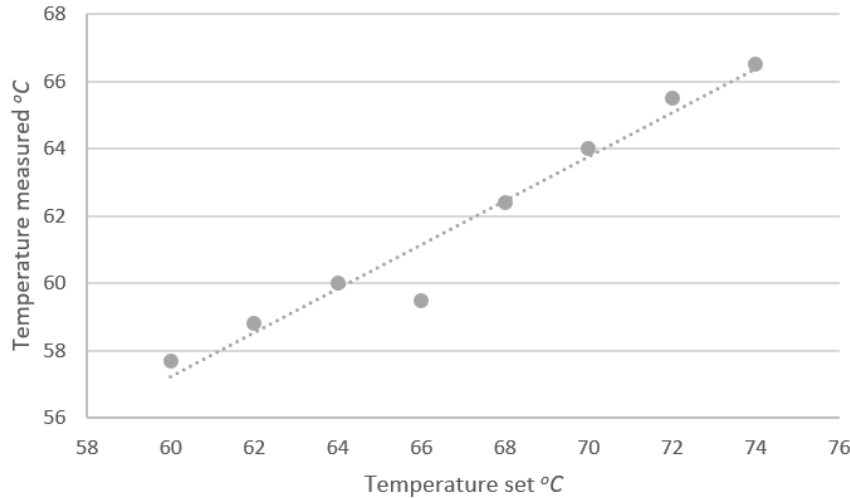


Figure 15 Temperature correction between the read reading from 10 Ω NTC thermistor and the set reading. The trendline follows equation $y = 0.655*x + 17.931$.

In the setup of the software the analog and digital ports are declared as outputs or inputs. Initial temperatures for the heater PCBs are read to function as reference and the Serial is started with baud rate of 9600. Serial messages are read character by character every time the loop-sequence cycles. The serial message is read as complete when '\n' character is received. Then the message is deciphered by checking whether it is a state or not.

All together there are seven states in the state machine. If heat is turned on, the PID-algorithm is always run to calculate new values for the PWM, not dependent on the state currently at. The default state into which the program always returns to is the INIT state, nothing is done in this state. CANCEL state sets the PWM outputs manual and turns their output to zero to stop the heating. HEAT_BOARDS state sets the Boolean value on that indicates that heat is to be calculated with every loop cycle and sets the PWM outputs automatic. INFO state just prints out the temperatures. SET_TEMP_UPPER and SET_TEMP_MIDDLE control the setpoints for the respective heaters, for the lower heater the correction algorithm is used.

READ_ASSAY state reads all the 96 PDs with and without the LEDs on. Because the temperature tends to rise a few degrees because the LEDs are kept on for a few seconds, the function first turns the PWM controlled outputs off. Then the function sets the LEDs on and keeps them on for 500 ms of time to allow

the LED light intensity to stabilize. After the 500 ms has passed the program reads the PD voltages five times to calculate the average, between each read is a 1 second delay. The selection between multiplexer is done inside a for-loop that loops all the multiplexer channels, the loop contains a switch that loops all the multiplexers. The readings are stored in a two-dimensional array. Then average is calculated by dividing the measurements with the number of measurements and data is displayed i.e. collected to a single string and printed to serial. Then all the arrays are emptied, because they are global variables, and all the multiplexers and channels read 15 times with 10 ms delay to read them empty. PWM is turned back on when the next Arduino loop commences.

To calculate the PID parameters for heater PWM control first the current temperatures are read from the PCBs. The voltage reading is corrected to an actual temperature by using correction values from manufacturer datasheet (see design document repository). After inputs have been calculated, gap between wanted and actual is calculated and decided whether to use aggressive or conservative gain values for PID-parameters. Last the PID-algorithm is computed.

4 Results

4.1 Heat uniformity

4.1.1 Top plate

Six iterations of the top plate were required to get the temperature uniformity across the plate consistent as well as to get the resistance to a suitable level. All the iteration rounds followed similar approach so that a $10\ \Omega$ NTC thermistor was placed in the exact midpoint of the plate and a trace was wrapped around the thermistor in different patterns. The first plate (UH_001) was just a figure of ever closing loop to midpoint and the last figure (UH_006) was a maze with trace gaps close to the midpoint slightly more distant apart from each other than in the edges. The hypothesis was that, as heat is measured in the middle, more the trace gaps are distant from each other, less heat will be generated. This was due to the fact that the plates faced near ambient air close to edges and all heat would be concentrated in the middle. To even out the distribution of heat, also a heat distributing silicon wafer was used in miriam. This product from CS Hyde Co (71-TCD-.062) is suitable also to create better seal between the tape covering the assay plate and the top cover.

The first plate (UH_001) had resistance of $1.6\ \Omega$ which was really low. It was not possible to use the plate with 12 V power supply with the electronic configuration miriam was designed to have. For the rest of the plate's measurements, how the temperature uniformity changed, were made by positioning a K-type thermocouple above different parts of the 96-well plate and closing the lid with heat wafer between cover and plate and keeping temperature on for two minutes and reading the thermocouple temperature reading. The temperature was adjusted to 90 degrees in all the cases. Below for reference is a heat map of UH_006 (Table 4).

Table 4 Heat map of UH_006 with temperature set to 90°C.

	1	2	3	4	5	6	7	8	9	10	11	12
A	81.0											90.0
B						84.7						
C												
D							84.0					
E									90.0			
F												
G			86.3									
H	84.0											94.0

The temperature uniformity was not perfect but the sixth iteration was used in the release version because the temperature uniformity of the top plate was not considered to be that important for assay purposes

as it was to prohibit condensation from forming. All the other upper heater temperature profiles were variations from the table above. What was quite strange in the heat map was that for some reason the temperature in the part of the plate that is closest to control electronics seems to be highest in UH_006, but for example for UH_004 this was vice versa. The difference between these two boards was that the for UH_004 the heating traces started from the edges of the PCB as for UH_006 the traces started from the middle. Even with not complete heat uniformity achieved in UH_006, the improvement in heat distribution was drastic between the iterations. For UH_002 the temperature difference was 20 degrees between the middle wells and the corner wells of a 96-well plate.

The different trace configurations are presented in Figure 16. The figure only depicts the first iteration UH_001 and the last UH_006 but all the iterations between were different versions of the layouts depicted in the figure. All the iterations contained a copper pill to even out the distribution of heat so that the pill was not connected to device ground. All the plates were printed on FR4 PCBs to make the plate slightly lighter as it is used in moving top cover. Aluminum was also considered, and one revision of UH_005 was made from aluminum, but the plate was ordered only printed one sided, which caused a short circuit on the line. The final UH_006 had trace resistance of 6.2Ω .

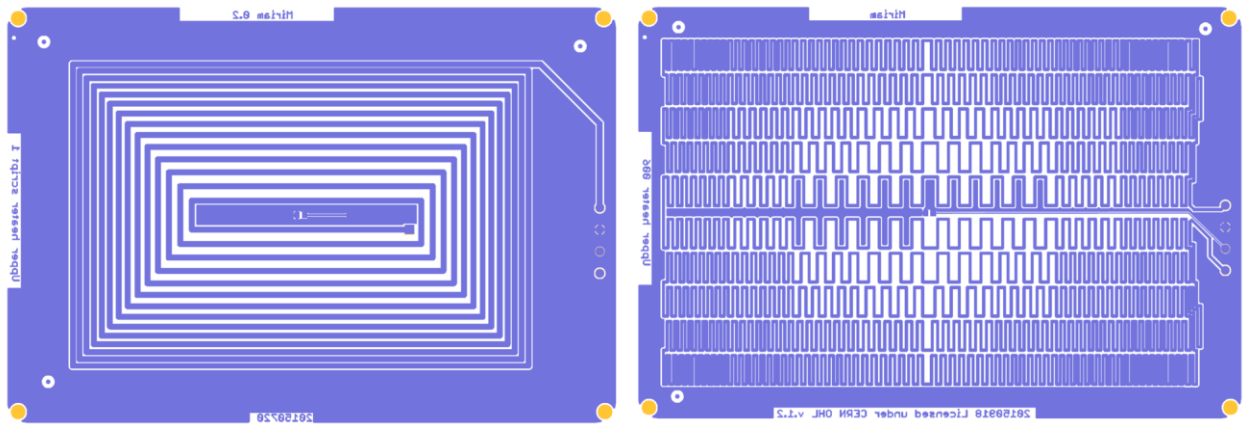


Figure 16 Illustrative example of the heat plate trace configurations. In the left is presented the bottom copper of the first revision (UH_001) and in the right the released one (UH_006).

4.1.2 Assay temperature plate

The lower heating board, to provide the assay suitable temperature of $55\text{--}65^\circ\text{C}$, followed similar kind of design iteration procedure as the top heating plate. The main difference between the heaters is that the lower heater contains 96 holes to house the assay plate. All together nine iteration rounds of different trace gaps in different parts of the plate were made. In Figure 17 is represented the first iteration of the

heating plate (LH_001) as well as the last (LH_009). All the iterations in between are different variations of these. The trace width in the figure is only 10 mils (0.254 mm). The difference between upper and lower heater is that the lower heater was double sided PCB with both the top and bottom copper containing similar kind of traces connected parallel with resistance of 8.4Ω . The material of the PCB was aluminum in order to provide enhanced heat distribution.

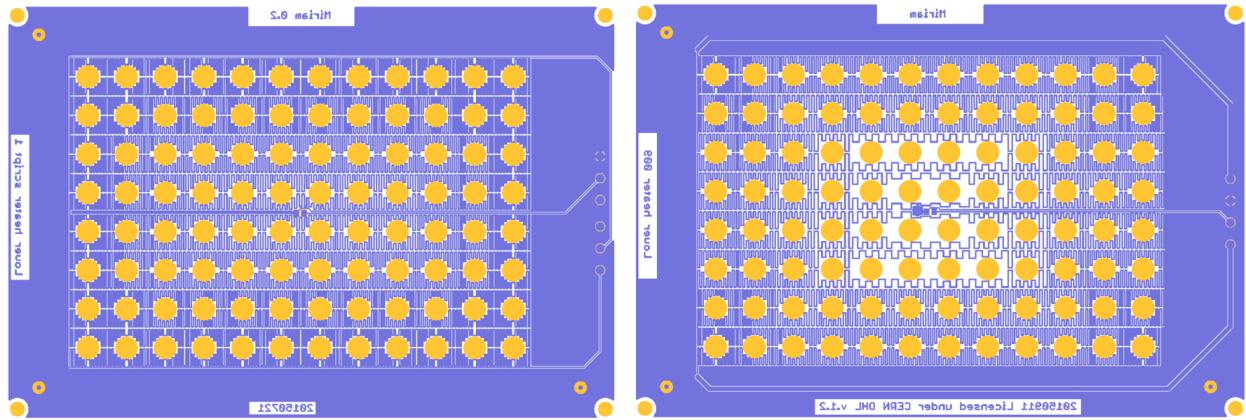


Figure 17 LH_001 and LH_009 bottom coppers respectively from left to right.

For all the plates a similar kind of temperature mapping was performed. A K-type thermocouple was placed in different wells of a 96-well plate to 50 μl of water. The temperature after opening and changing the measurement point was upheld for 5 minutes before recording the temperature. In the final iterations, also including LH_009, a heat distributing silicon wafer was placed between upper heater and assay plate to even out the distribution of heat and to better seal the wells. In Table 5 is represented the heat map for LH_009.

Table 5 LH_009 temperature profile with CS Hyde Co product 71-TCD-.062 placed in between the top heater and assay plate. The temperature set was 65°C .

	1	2	3	4	5	6	7	8	9	10	11	12
A	64.7											62.5
B												
C					65.0							
D												
E						64.6						
F												
G							65.0					
H	63.2											62.7

In the final iteration, LH_009, the heat was distributed evenly across the plate. For some reason the temperature was two degrees lower in the corner where the control electronics are placed, quite unlike

for the upper heater where the situation was vice versa. Possibly due to the fact that in the lower heater the traces used in heating started from the other edge of the PCB as was the case with upper heater. The improvement to first iteration (LH_001) was quite drastic. For LH_001 the temperature difference between the middle and the edge of the plate was between 10 to 20°C, depending on the corner (Data not shown). The mechanical setup changed quite drastically between the iterations since the box was changed from a wooden case to 3D printed final case which also affected the temperature profile.

4.2 Fluorescent detection

4.2.1 First revision

The first iteration of the LED PCB was made to house two different kinds of LEDs. Both of the LEDs were angle mount SMDs with specification listed in the Table 1. The LEDs were aligned so that the first four rows had the LED AA4040QBS/D (L1) and the last four rows the KA-2810AQBS-G (L2). The LEDs were in series of three similar LEDs connected to a series resistor of 68 Ω. The main difference between the LEDs was the case size, otherwise the optical as well electrical properties were quite similar. The luminous flux was slightly stronger with L2 than L1, 300 mcd and 220 mcd with 20 mA forward current respectively.

In the first draft of the sensor board two different RGB sensor PDs were used. The two used PDs were from the same manufacturer, from the same family and thus they had similar PCB footprint. Different was the peak sensitivity wavelength, for green the peak was 550 nm (CLS15-22C/L213G/TR8, PD1) and for red PD 620 nm (CLS15-22C/L213R/TR8, PD2). When looking at the calcein emission spectrum the green PD is ideal, the sensitivity peak is only 30 nm from the emission peak of calcein. But when comparing the sensitivity spectrum of the PD2 to LED light spectrum from either of the LEDs, there is still 10% sensitivity left at 461 nm than the red PD has only 1%. The two different sensors were placed on the PCB so that the first six columns contained PD1 and the latter six columns PD2.

The two different combinations were tested with emission filter GAM-388 between the sensor PCB and the LED PCB. The used fluorescent solution was calcein in water diluted in four different concentrations. The volume was 20 ul per well. Background was measured with an assay plate of all the wells having water of 20 ul. The different concentrations and background were pipetted each to fill a 96-well assay plate that was read whole. The black background was removed from the fluorescent reading first measuring the sensor response in dark and then subtracting the reading from the one with light source on. The measurement was repeated 3 times and an average was calculated.

In the first iteration, PCBs were assembled in a wooden box to ensure darkness in the measurement area. In Figure 18 is shown the assay result with an average of two best performing wells from each measurement area. The SG/BG ratio has been counted to each average using water plate as background. From the results, it is obvious that the second LED works drastically better than the first LED not dependent on the PD. The bigger L1 works to some extent with the green sensitive PD, SG/BG rises close to 4, but the L1 does not work at all with the red sensitive PD. The second LED works with both of the selected PDs, but the response is drastically higher with green sensitive PD1 so that the signal seems to saturate already at 100x initial concentration.

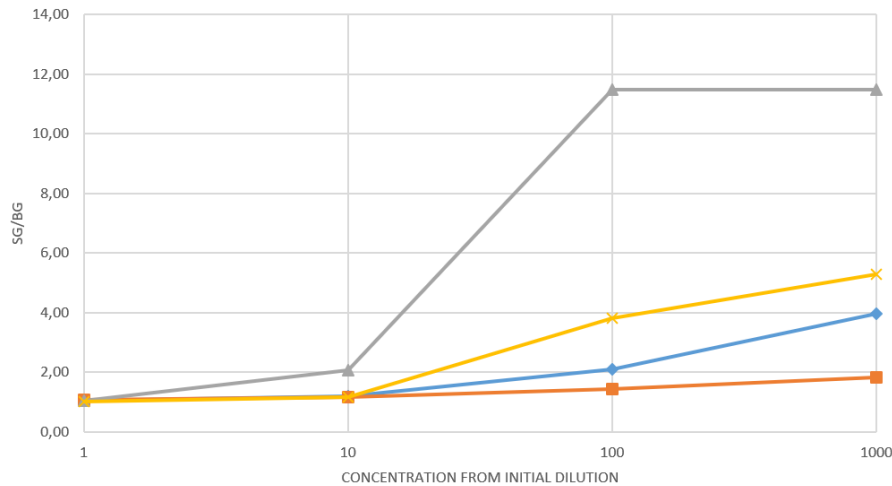


Figure 18 Calcein dilution effect on fluorescent reading by using two different LEDs and two PDs. Blue diamonds: L1, PD1; red squares L1, PD2; gray triangles L2, PD1 and yellow crosses L2, PD2.

The second LED is bound to work better due to the height of the component. The L1 was 4 mm in height and the light originates from a height of 2.6 mm as with L2 the total height of the component was only 0.8 mm. This means that the surface of the liquid in well must be 2.2 mm higher with L1 than with L2. Because miriam contains also no optical elements to collect light, 2.2 mm is a very long distance for light to travel unscattered. The green PD performance was not a surprise because the sensitivity peak wavelength is so close to calcein emission peak wavelength. A small surprise though was that the LED light did not leak that extensively to measurement channel, a dark reading with LED off the PD voltage was around 20 rfu (relative fluorescence unit) as for L2 on, the reading was 120 rfu.

The SG/BG varied drastically depending on the position of the well on the 96-well plate even though the solution in each well was the same. This was probably due to the fact that the first PCBs contained hand soldered components and hence there were some misalignments in the placement of the components. In

optics the alignment of the components is crucial for the optical performance. A bonus, as well as a downside, in miriam is that there are no lenses. A bonus due to the fact that that would be an additional component to align in the light path but also a hindrance because lenses collect and concentrate light. The PCBs contained also few components that did not work at all probably due to soldering defects. During the measurements it was noticed that the readings could have been improved with a slight modification to the firmware. The PD signal lines had some internal capacitance and after the PD had been illuminated, especially with fluorescent reading, the PD measurement channel stored some voltage for the next reading. It was possible to circumvent this problem by reading the channels in the dark for multiple times after one illuminated reading.

The data was sufficient to select the best performing LED and PD pair for the next iteration round. Selected was the second LED which was also ideal for the setup due to dimensions, especially the height of the component. From PDs the green one was selected even though the red one gave more linear response as the green one seemed to saturate already at 100x initial dilution. It was assumed that the saturation could be taken into consideration when selecting a suitable resistor for the LED PCB.

4.2.2 Second revision

The second ordered LED board contained only the selected LEDs (KA-2810AQBS-G). The board was intended to test out the best resistor to be used to properly set the light intensity. The different resistor arrays ordered were between $32\ \Omega$ and $470\ \Omega$. $68\ \Omega$ resistor is the first appropriate resistor to ensure the 30 mA forward current for the LED to have the strongest light intensity. Peak forward current for the LED would have been 150 mA with $1/10$ duty cycle and 0.1 ms pulse width. It was considered to shorten the measurement time with LED on to 0.1 ms in order to use a resistor with less resistance to gain a stronger reading, if a stronger light intensity would have been required.

The second iteration of the sensor PCB contained only the selected green sensitive RGB PDs and was ordered fully assembled by the PCB manufacturer. The LED boards were also assembled by the PCB manufacturer automatically excluding the resistor arrays, which were hand soldered. The PCB layout contained a few faults which led to short circuits and those shorted LEDs had to be hand soldered off. For testing purposes eight similar resistor arrays were populated per board. The best performing resistor LED combination was with $181\ \Omega$ resistor (Figure 19).

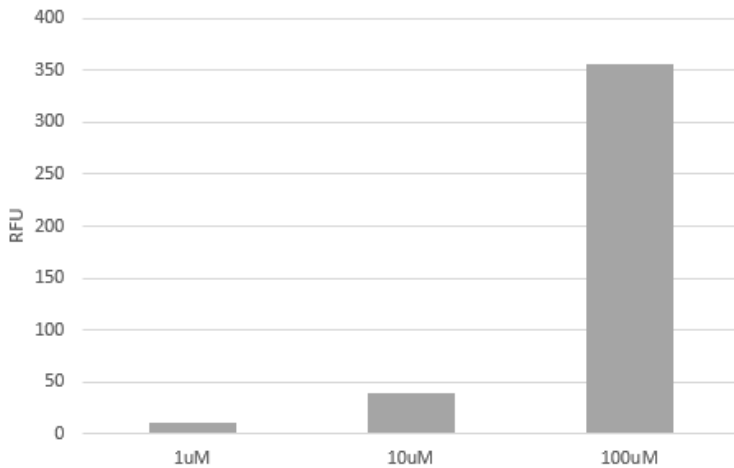


Figure 19 Dark background corrected fluorescent measurement readings from three different calcein concentrations, sample volume 10 ul. Upper heater temperature set to 90°C and lower to 63°C. Concentration represented on the x-axis is Miroculus assay template concentration in micro molar range.

The $181\ \Omega$ was a tradeoff between light intensity and generated heat. The reading lasted for three seconds so that the LED was first on for 0.5 seconds, PD voltage reading was performed and LED turned off. The reading was performed three times in a row and the average was used. The SG/BG ratio was improved slightly with using lower resistance, but the downside was that the LEDs started to generate vast amounts of heat that could not be handled any more with PWM controlled lower heating board. The temperature rise for the $68\ \Omega$ resistor was 2°C after repeating the reading three times even with turning PWM heating off. The heat generated lowered with resistance increase and $181\ \Omega$ resistor was selected as the best candidate. The lower light intensity was also to prohibit photobleaching phenomenon of the fluorophore.

The working LED and PD combination with $181\ \Omega$ LED resistor was also used to test the performance on whole LAMP assay. Multiple trials were performed before the first successful amplification reaction was recorded. In Figure 20 is presented the first successful LAMP test performed with the second iteration of miriam. Two different concentration of micro-RNAs to be amplified were used in the reaction (termed: high and low) and water background. The assay used Miroculus patented micro-RNA amplification technology and the reagent volume was 20 ul. Three replicas per sample were used and they were positioned to different parts on the 96-well plate quite close to the center of the assay plate. The used temperature in the reaction was set to 90°C for top heater and 65°C to lower heater.

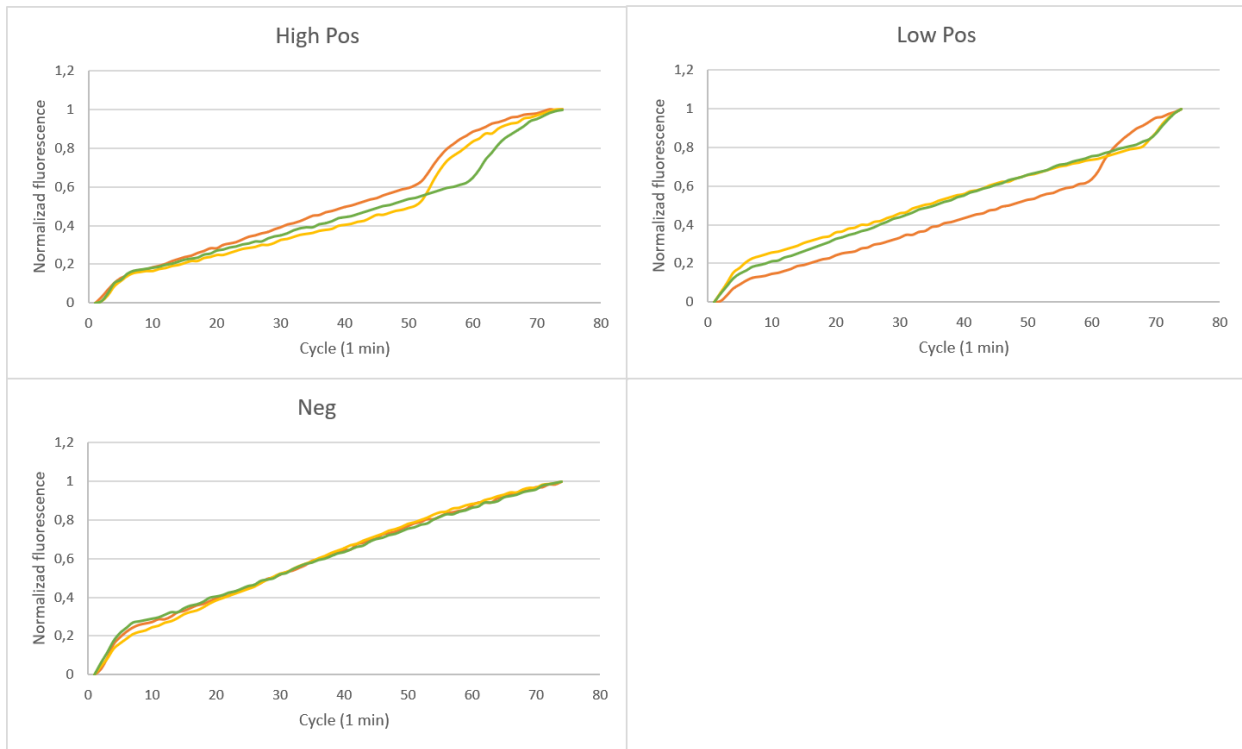


Figure 20 LAMP assay performed on the second iteration of LED and sensor boards. The used volume was 20 μ l and the assay uses Miroculus patented micro-RNA amplification technology using three replicas of three different concentrations of micro-RNA as template: High pos, high micro-RNA concentration; Low pos, low micro-RNA concentration; Neg, no micro-RNA template.

The positive reaction is visible from the start of the exponential phase of fluorescence. All samples with micro-RNA sample in them gave positive response. The relative position of the well on the plate had an effect on the start of the exponential phase even though the concentration was the same between the three replicas. In an ideal case, all the replicas would have had simultaneous start of the reaction, but in this first try at least the high concentrations gave response first before the low ones and the no micro-RNA wells gave a flat signal. The difference in the exponential fluorescence increase start cycle was probably due to slight temperature variation between the middle of the plate when compared to the edges of the plate. See section 4.1.2 Assay temperature plate.

An interesting find also was that even the no micro-RNA template reactions had a linear rise in fluorescence reading throughout the assay. It seems that calcein fluorescence has a positive fluorescent effect due to incubation in high temperatures. Probably the salts in the assay liquid start to react with calcein. Calcein has been noticed to increase the fluorescence during prolonged incubation (Williams et al. 2010). The quite rapid rise of fluorescence in the beginning of assay is also an interesting phenomenon not previously described in literature.

4.2.3 Final iteration

The final tests with the optics were performed with the release version of miriam. The mechanical setup was the final version of the 3D printed case and the temperature PCBs were the UH_006 and LH_009 that ascertained almost uniform temperature profile across the plate. For heating purposes, also the silicon wafer heat distributor was used between the top heating plate and the 96-well plate. The assay was also ran using the firmware that allowed communication between Miroculus cloud service and miriam so that all the communication between miriam and the user happened via cloud. In Figure 21 is represented the assay result using two replicas of micro RNA template compared to negative background.

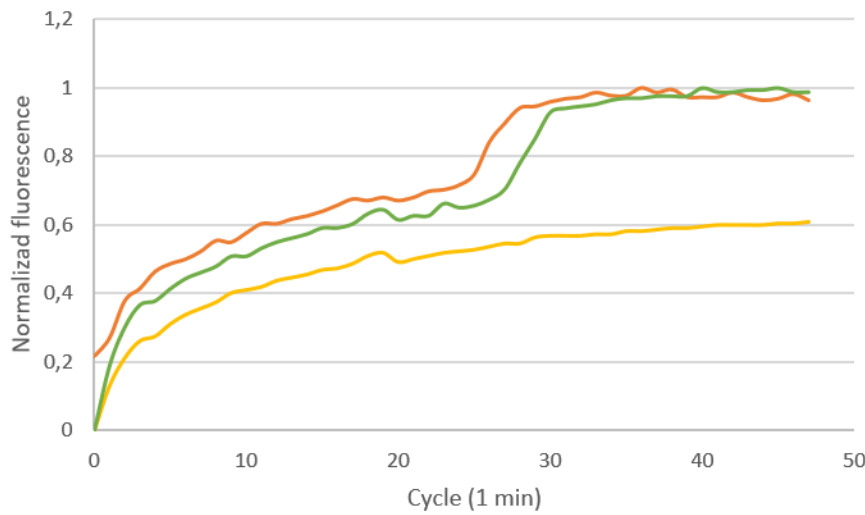


Figure 21 LAMP assay performed on the final version of miriam. The used volume was 10ul and the assay uses Miroculus patented micro-RNA amplification technology. Two replicas of positive micro-RNA sample were used and compared to no micro-RNA sample. The assay wells were positioned close to middle of the 96-well plate.

In the results it can be seen that the rise cycles are only 3 minutes apart from each other meaning that the temperature variation between the samples did not so drastically affect the assay.

4.3 Shield

All together seven shield iterations were made. First there was a comparison between the WIFI and Bluetooth module. Miroculus decided to use WIFI module for the ease of use of the module. It was possible to connect the module to a WIFI in the laboratory and hence use a computer to directly connect the IP address miriam acquired to access the TCP/IP communication. The second benefit of the WIFI module was the ability to create its own WIFI which could be utilized in low resource settings. With the WIFI module miriam was able to reach up to 20 meters in distance from the device with its own WIFI hotspot as the communication with the Bluetooth module the distance was limited to 10 meters.

Difference also between the shield iterations was the addition of 3.3 V DC/DC converter. The first iterations of shield used Arduino provided 3.3 V power supply, but it was not sufficient to provide enough power to the WIFI module. The next used ATX connector 3.3 V output for the WIFI module which worked really well. For the final released version Miroculus wanted to get rid of the need for ATX connector dependency and hence the SHIELD_007 was designed with 3.3 V DC/DC converter.

5 Discussion

5.1 Heating

Trace heating proved to be an efficient means of providing assay suitable conditions for the LAMP reaction to occur as well as to stop condensation from forming to the seal tape of a 96-well plate. There remained still a small temperature difference between the edges of the plate and the midpoint of the plate. The temperature was also higher on one edge of the PCB from the other edge of the PCB. The origination point of the heating traces had higher temperature as the opposite edge. For the top heater the temperature differences led to some condensation of liquid to the well sealing tape on the edges of a 96-well plate even with the use of silicon heat distributing wafer.

New iteration rounds would be required to even out the distribution of heat. It was noticed that the best way to design better heat uniformity plates was to design a bulk of different options, order them and test them. This was due to the fact that a PCB order from the manufacturer lasted on an average of two to three weeks. In future it might also be suitable to utilize software meant for heat mapping. One downside in such an approach is the difficulty in measuring the heat from the wells of a well plate evenly. Harm is also caused because measuring temperature of the wells in ambient air would not depict the real situation.

One way to improve the heating would be to change the N-channel MOSFET to an ideal diode. The voltage drop of an ideal diode is considerably less than with using a MOSFET control. This would also lower the heat generated by the switch. The footprint of an ideal diode could also be a bit smaller making it possible to house more ideal diodes on the shield.

One way to improve the heat distribution would also be to use multiple thermistors on the heater PCBs. Initially the lower heater contained two NTC thermistors, one for each side of the PCB that each had own ADC channel for temperature reading. This had no additional value, because the PWM controlled 12 V line had only one input to the PCB. Both the bottom and the top copper of lower heater PCB also had to be connected parallel to lower the resistance to make the temperature increase faster. Multiple thermistors and multiple 12 V PWM controlled lines could also aid in the heat uniformity.

By controlling the heat on the PCB in five segments, one segment in the middle and each corner being controlled separately could aid to even out the temperature differences across the PCB. This way the current to each segment could be lowered below 1 A and an ideal diode like MAX40200 from Maxim Integrated could be used (Maxim 40200). The voltage drop of MAX40200 using 1 A load is only 85 mV and

the diode comes in a handy SOT23-5 package that is very small in compared to the N-channel MOSFET (TO-263) currently in miriam. The voltage drop of the used MOSFET is 1 to 1.25 V.

5.2 Optics

The first version of miriam was made to house optics for Miroculus used fluorophore calcein. Calcein is an organic fluorophore and reacts to manganese ions released during the LAMP reaction becoming fluorescent. Calcein was an easy fluorophore to work with and its fluorescence was quite robust, the samples did not lose their fluorescent properties during time.

In the released version of Miroculus black silkscreen was used on white soldermask. This was to make the surfaces reflective to boost the LED light collection to the sample. In the next revision of miriam, the situation should be reversed. Black soldermask could remove the light scattered to the PDs. By having just the LED on by itself, PD reading was 100 rfu higher than the dark background of PD measurement. This means that some LED light is collected by the PDs.

One of the most used fluorophores in the field of biotechnology is SYBR green. SYBR green emission and excitation peaks are quite close to calcein (490 and 530 nm respectively). As calcein becomes fluorescent with the presence of manganese ions, SYBR green becomes fluorescent binding to double stranded DNA. This makes it more suitable to be used in assays related to DNA amplification because a positive reading of fluorescence is bound to originate from double stranded DNA. When designing miriam, it was also assumed that SYBR green could be utilized as a fluorophore in the assays. Positive SG/GB ratios were not achieved with miriam using SYBR green in none of the tests performed. It might be that the internal fluorescence of SYBR green is not as strong as with calcein possibly due to the fact that fewer ions are fluorescent.

Another fluorescent dye used by Miroculus is called BCECF. BCECF excitation peak is at 492 nm and emission peak at 510 nm. BCECF is mainly an electrochemical dye. The change of pH during an assay reaction makes BCECF fluorescent, more alkaline the reaction is, higher is the fluorescence. BCECF was found after SYBR green was noticed not to work with miriam. With BCECF there was a slight indication that with assay buffer modification, it could be made possible to use BCECF with miriam. Shamefully there was not enough time to optimize the assay as Miroculus wanted to release the product.

One way to enhance the fluorescent optics would be to create a plane between the LED and PD PCBs that would contain the optical filter and 96 lenses to collect light from the sample more efficiently. This kind of

an optical plane would increase the cost of miriam quite drastically but could improve collection of light before the PDs.

The components used in the optical setup are already five years old. By updating the components to new ones more sensitivity could be achieved, especially with the PD used. The $3.9\text{ M}\Omega$ resistor was also the first one to try and because that resistor seemed to work with calcein sufficiently, no further work was done to optimize the inverting operational amplification gain. It could be that by increasing the resistance the SG/BG ratio could be improved.

By searching new components, also new LEDs could be found that would enable the usage of other fluorophores. As said before, the shoulder in calcein excitation spectrum at 460 nm is very beneficial for blue LEDs. The LED used in miriam is doped with InGaN (Indium gallium nitride) and hence the light intensity peak is at 461 nm. Another blue LED with different doping material could overcome the problem of exciting fluorophores without an excitation shoulder at 460 nm. Another LED could have a green doping material e.g. Gallium(III) phosphide that would be ideal for SYBR green excitation, the downside would be the light leakage to emission channel. Finding these LEDs angle mounted could be an issue. There are some alternatives like Bivar Inc 500 nm peak right-angle mount SMD LED SM1204PGC that could be tested.

5.3 Control interface

The embedded software on miriam is written in C++ using Arduino IDE. All three versions follow similar kind of an API, the heating, as well as LED and PD control, work the same way. What is different is how the interaction between the user and miriam is realized. Two helper C# programs are released in the repository containing the design documents for miriam. One is a direct serial communication software using the USB connection of Arduino and the second C# program uses the ESP12 WIFI module of communication.

The C# programs and the source codes are available in the design document repository. There is no reference software available for the communication between Miroculus cloud and miriam, only communication protocol is described in the repository.

The embedded software is a result of trial and error and hence it contains quite many lines of unused code. The internal references in the C++ code are also not documented nor written quite clear. All three source codes would require an extensive cleanup to make them clearer. The PID algorithm used could also be updated to the latest version of the Arduino PID control utensil.

One fault in the firmware is that the long-lasting fluorescent measurement reading interrupts the PWM control of the heaters. Because one LED reading lasts for approximately five seconds, the heating PWM output is stuck to the last value it was adjusted to have before measuring the PD signal. This is due to the sleep commands in the LED control. We want to keep LED illumination on for 500 ms before reading the PD voltage and because the sleep command is given in the same loop that runs the PID algorithm, the loop during fluorescent measurements gets stuck. A simple way to correct this would be to write an own sleep algorithm using a while loop and Arduino clock frequency to calculate when 500 ms has passed. Shamefully there was not enough time to realize this approach before miriam was to be launched.

5.4 Electronics

The control electronics of miriam are quite simple and robust due to all the possibilities Arduino Mega provides. The control electronics could have been miniaturized for example by getting rid of Arduino Mega and this way utilizing cheaper processor like 32-bit Cortex M0 instead of the 8-bit Atmega2560 which is quite expensive. To gain a government approval, this would have probably been a must. But to launch a product to open source market, it is better to use the available tools already present for the community. Designing a simple circuit that supports the community accepted standard is then a better option especially due to no dimension constraints currently in miriam.

The next thing to develop in the control electronics of miriam is to get rid of the too extensive ATX connector. In the last miriam the ATX power supply has already been replaced with a power converter and ATX connector that only creates all the ATX required voltages. This was the fastest option to go from idea to a fully functioning product. The last version of miriam shield only requires 12 V input and it creates all the other voltages it requires. Hence the ATX connector can be replaced with a suitable 12 V power jack that can be aligned directly on top of the Arduino USB jack.

One thing to consider in the shield electronics are the pull-down resistors for 5 V and 3.3 V lines. Both contain a $4.12\ \Omega$ pull down resistor to make sure constant line voltage. Both lines do not need the pull-down resistor, only 3.3 V line that is converted from 5 V, would need a constant pull-down if that would be the case. But both pull-down resistors could be removed in the next version of control electronics and thus the power demand of control electronics could be lowered.

6 Conclusions

In this thesis is presented the world's first open source isothermal DNA or RNA amplification hardware. miriam is the product of collaboration between Miroculus and Arduino. The initial driver behind miriam was to cut down the price of DNA amplification instrumentation and in this miriam succeeded. The production costs per piece are below 200\$ as the qPCR capable instrumentation price ranges from 4500\$ to tens of thousands.

The reason for the low price of miriam is the lack of temperature cycling components. miriam only provides isothermal conditions for assay protocols that can multiply DNA or RNA in stable temperatures. The heating is realized with trace heating so bare PCBs are the only thing required. The lack of optical components also lowers the price of miriam. The real time detection of the amplification reaction happens with 96 LEDs in combination with 96 PDs separated with an emission filter used in theatrical illumination purposes. miriam can run assays with industry accepted standard 96-well plate.

The instrument has been tested to function in micro-RNA based LAMP amplification protocols used by Miroculus. Currently miriam can be used in research use only settings as no governmental approvals have been acquired for miriam. The design documents are freely available to public under Github repository <https://github.com/miroculus/Miriam>.

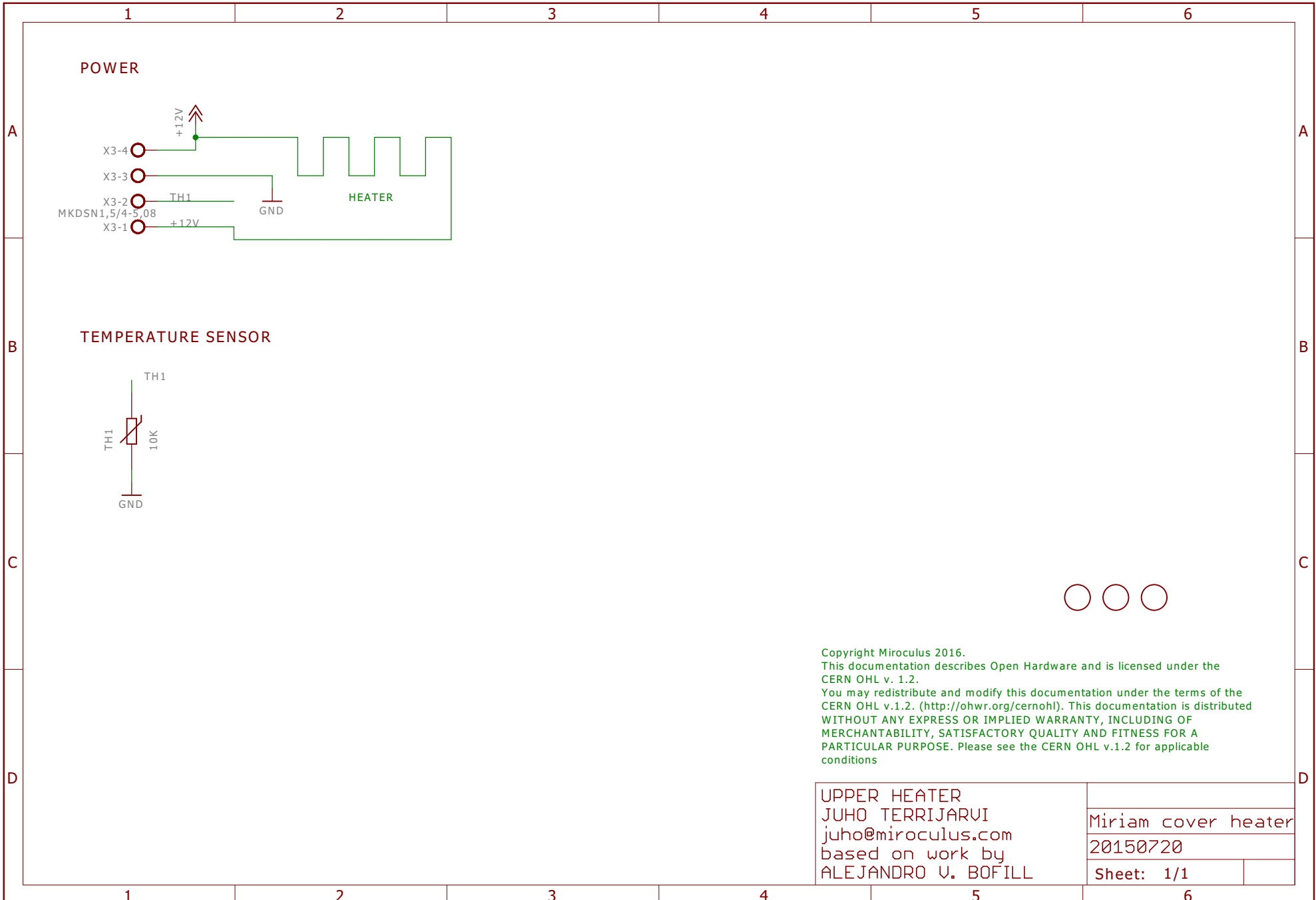
References

- Abacus Diagnostica, GenomEra technology, <https://www.abacusdiagnostica.com/technology/>, read 7.4.2019.
- BioRad, Introduction to qPCR Instrumentation, <http://www.bio-rad.com/en-fi/applications-technologies/introduction-qpcr-instrumentation?ID=LUSO5YMNI>, read 7.4.2019.
- Boehm C, Use of polymerase chain reaction for diagnosis of inherited disorders, Clin. Chem. 1989, 1843-1848.
- Chai, A fast, accurate, and portable real-time PCR machine, <https://www.chaibio.com/openqpcr>, read 7.4.2019.
- Deepak S, Kottapalli K, Rakwal R, Oros G, Rangappa K, Iwahashi H, Masua Y and Agrawas G, Real-Time PCR: Revolutionizing Detection and Expression Analysis of Genes, Current Genomics 2007 234-251.
- European commission, In vitro diagnostic medical devices, https://ec.europa.eu/growth/single-market/european-standards/harmonised-standards/iv-diagnostic-medical-devices_en, read 7.4.2019.
- Gordon M, Ha T and Selvin R, Single-molecule high-resolution imaging with photobleaching, Proc Natl Acad Sci U S A, 2004, 6462–6465.
- Liu W, Huang S, Dong D, Yang Z, Tang Y, Ma W, He X, Ao D, Xu Y, Zou D and Huang L, Establishment of an accurate and fast detection method using molecular beacons in loop-mediated isothermal amplification assay, Scientific Reports 2017.
- MAX40200, Maxim Integrated,
<https://www.maximintegrated.com/en/products/analog/amplifiers/MAX40200.html>, read 15.4.2019.
- NIH, 2015, Polymerase Chain Reaction (PCR), <https://www.genome.gov/10000207/polymerase-chain-reaction-pcr-fact-sheet/>, read 7.4.2019.
- Notomi T, Okayama H, Masubuchi H, Yonekawa T, Watanabe K, Amino N and Hase T, Loop-mediated isothermal amplification of DNA, Nucleic Acids Res. 2000.
- OpenPCR, Open source PCR, <https://openpcr.org/>, read 15.4.2019.

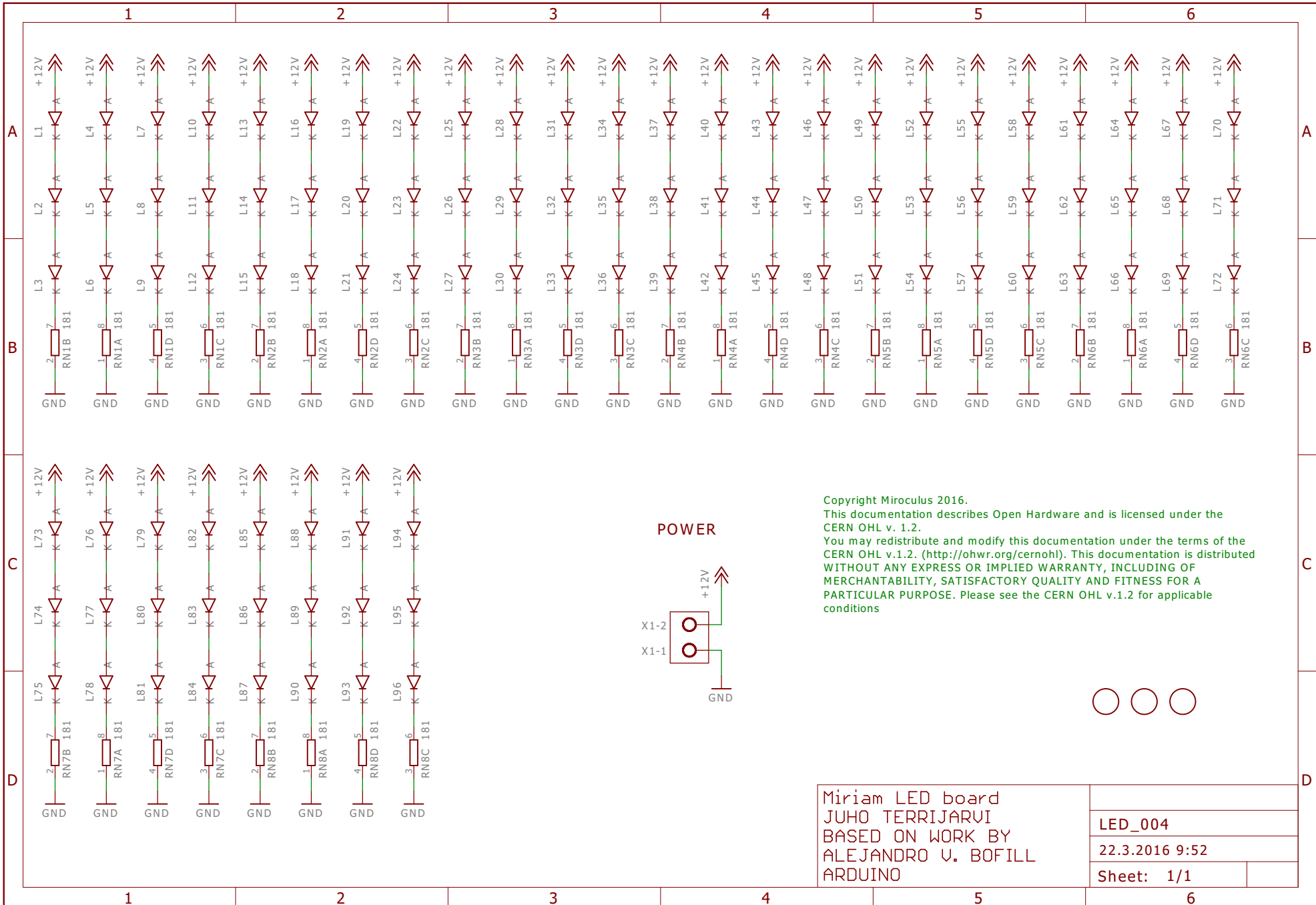
- ScienceDirect, Reverse Transcription Polymerase Chain Reaction, 2017,
<https://www.sciencedirect.com/topics/neuroscience/reverse-transcription-polymerase-chain-reaction>,
read 7.4.2019.
- Thanthrige-Don N, Lung O, Furukawa-Stoffer T, Buchanan C, Joseph T, Godson D, Gilleard J, Alexander T and Ambagala A, A novel multiplex PCR-electronic microarray assay for rapid and simultaneous detection of bovine respiratory and enteric pathogens, *J Virol Methods*, 2018.
- Tuladhari E, Hazeleger W, Koopmans M, Zwiering M, Beumer R and Duizer E, Residual Viral and Bacterial Contamination of Surfaces after Cleaning and Disinfection, *Appl Environ Microbiol*, 2012.
- Yu F, Ding Y, Gao Y, Zheng S and Chen F, Fluorescence enhancement effect for the determination of DNA with calcein–cetyl trimethyl ammonium bromide system, *Analytica Chimica Acta*, 2008 195-200.
- Williams T, Day I and Serpell L, The Effect of Alzheimer's Ab Aggregation State on the Permeation of Biomimetic Lipid Vesicles, *Langmuir*, 2010.

Attachments

- Upper heater (UH_006) schematic
- Upper heater (UH_006) BOM
- Lower heater (LH_009) schematic
- Lower heater (LH_009) BOM
- LED (LED_003) schematic
- LED (LED_003) BOM
- Sensor (sensor_002) schematic
- Sensor (sensor_002) BOM
- Shield (shield_007) schematic
- Shield (shield_007) BOM



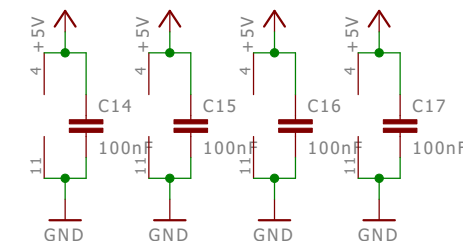
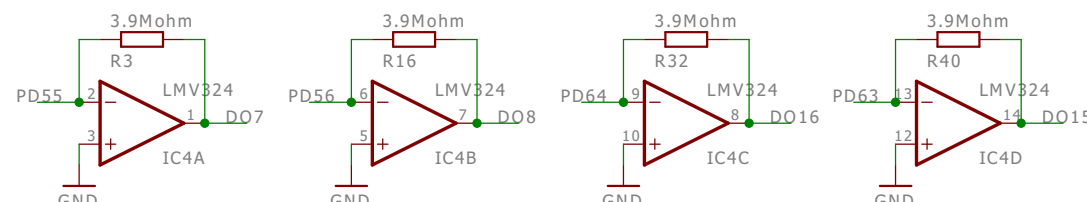
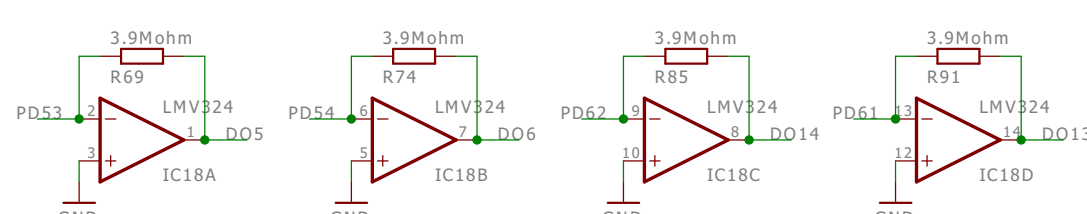
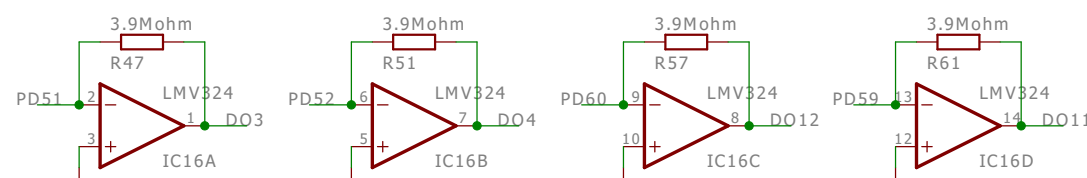
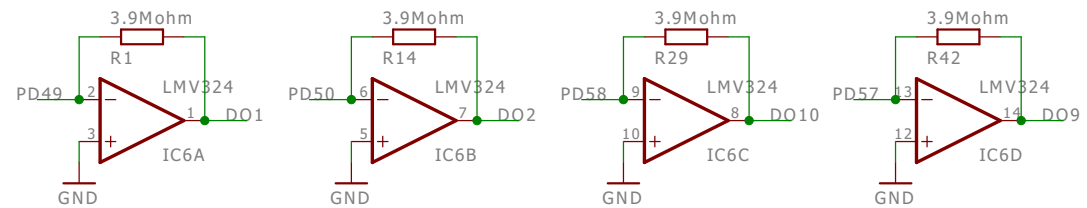




Copyright Miroculus 2016.
 This documentation describes Open Hardware and is licensed under the CERN OHL v. 1.2.
 You may redistribute and modify this documentation under the terms of the CERN OHL v.1.2. (<http://ohwr.org/cernohl>). This documentation is distributed WITHOUT ANY EXPRESS OR IMPLIED WARRANTY, INCLUDING OF MERCHANTABILITY, SATISFACTORY QUALITY AND FITNESS FOR A PARTICULAR PURPOSE. Please see the CERN OHL v.1.2 for applicable conditions



1 2 3 4 5 6



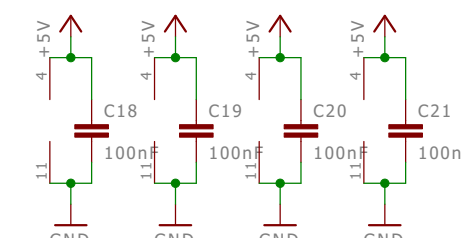
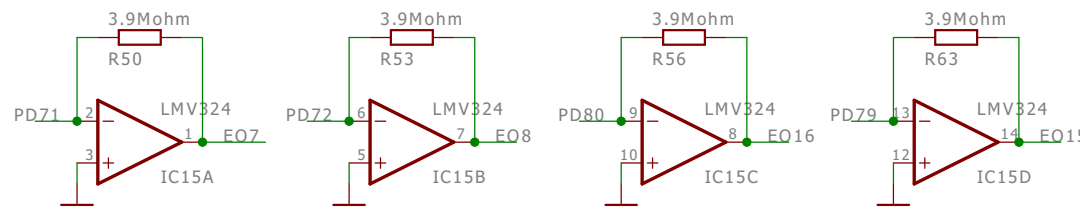
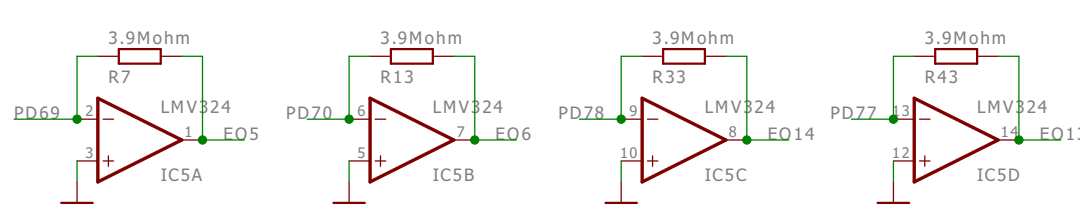
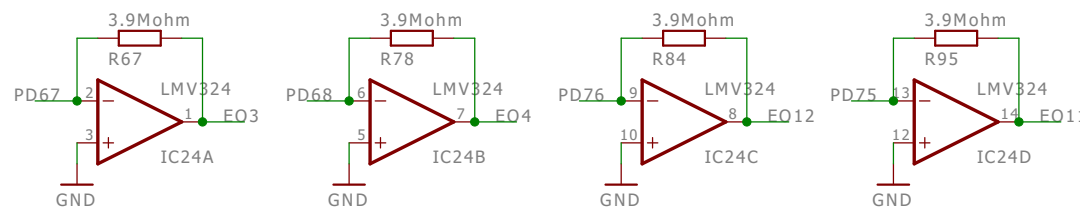
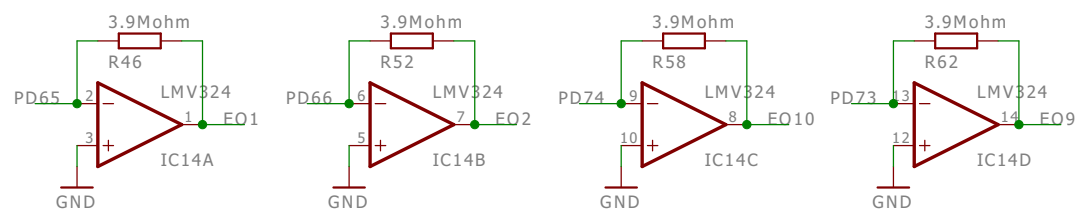
Copyright Miroculus 2016.
This documentation describes Open Hardware and is licensed under the
CERN OHL v.1.2.
You may redistribute and modify this documentation under the terms of the
CERN OHL v.1.2. (<http://ohwr.org/cernohl>). This documentation is distributed
WITHOUT ANY EXPRESS OR IMPLIED WARRANTY, INCLUDING OF
MERCHANTABILITY, SATISFACTORY QUALITY AND FITNESS FOR A
PARTICULAR PURPOSE. Please see the CERN OHL v.1.2 for applicable
conditions

SENSOR BOARD V2
JUHO TERRIJARVI
BASED ON WORK BY
ALEJANDRO U. BOFILL
ARDUINO

AMPLIFIERS 4
sensor_002
11.4.2016 20:50
Sheet: 1/1

1 2 3 4 5 6

1 2 3 4 5 6



Copyright Miroculus 2016.
This documentation describes Open Hardware and is licensed under the
CERN OHL v. 1.2.
You may redistribute and modify this documentation under the terms of the
CERN OHL v.1.2. (<http://ohwr.org/cernohl>). This documentation is distributed
WITHOUT ANY EXPRESS OR IMPLIED WARRANTY, INCLUDING OF
MERCHANTABILITY, SATISFACTORY QUALITY AND FITNESS FOR A
PARTICULAR PURPOSE. Please see the CERN OHL v.1.2 for applicable
conditions

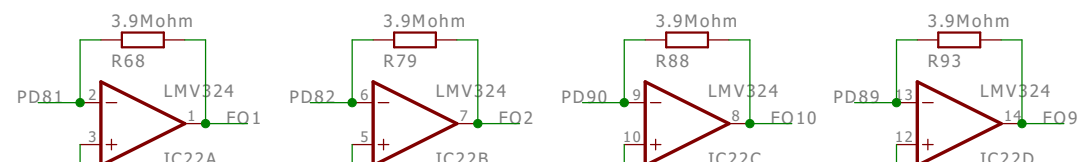
SENSOR BOARD V2
JUHO TERRIJARVI
BASED ON WORK BY
ALEJANDRO V. BOFILL
ARDUINO

AMPLIFIERS 5
sensor_002
11.4.2016 20:50
Sheet: 1/1

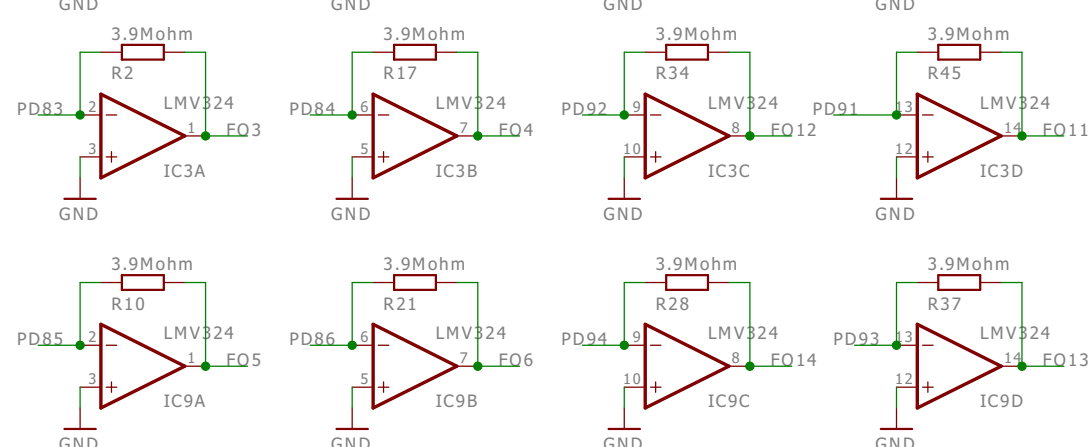
1 2 3 4 5 6

1 2 3 4 5 6

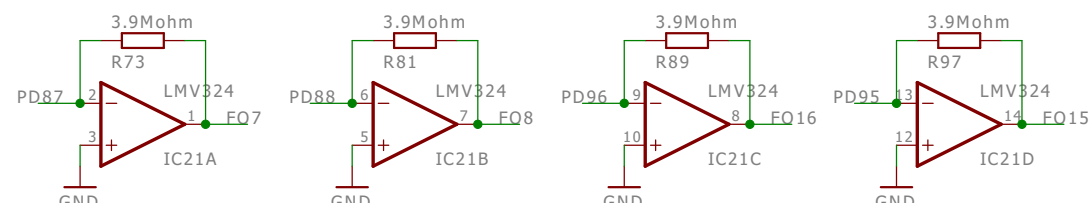
A



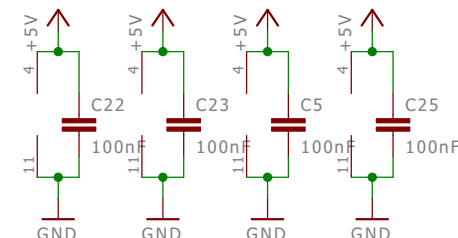
B



C



D



Copyright Miroculus 2016.

This documentation describes Open Hardware and is licensed under the CERN OHL v. 1.2.

You may redistribute and modify this documentation under the terms of the CERN OHL v.1.2. (<http://ohwr.org/cernohl>). This documentation is distributed WITHOUT ANY EXPRESS OR IMPLIED WARRANTY, INCLUDING OF MERCHANTABILITY, SATISFACTORY QUALITY AND FITNESS FOR A PARTICULAR PURPOSE. Please see the CERN OHL v.1.2 for applicable conditions

SENSOR BOARD V2
JUHO TERRIJARVI
BASED ON WORK BY
ALEJANDRO V. BOFILL
ARDUINO

AMPLIFIERS 6

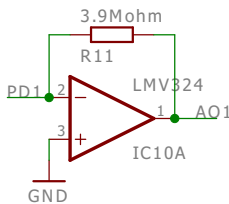
sensor_002

11.4.2016 20:50

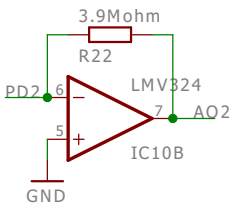
Sheet: 1/1

1 2 3 4 5 6

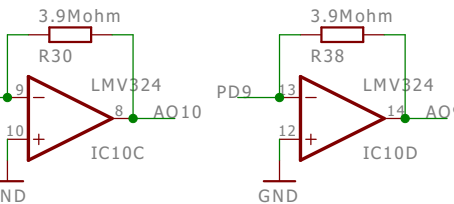
1



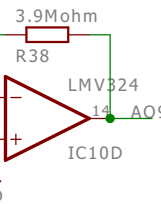
2



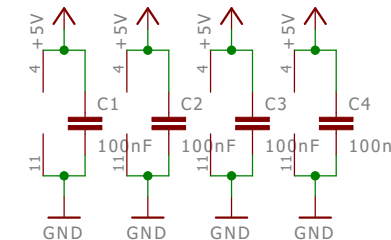
3



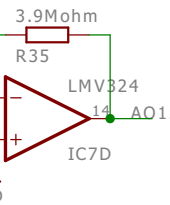
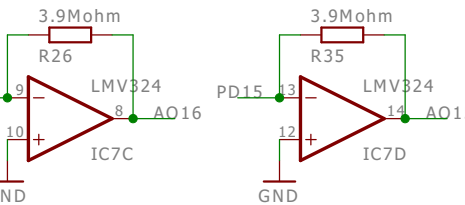
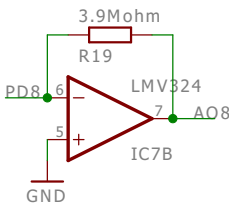
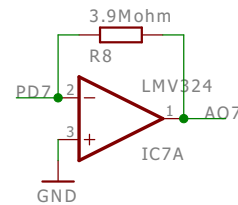
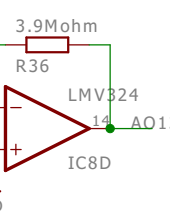
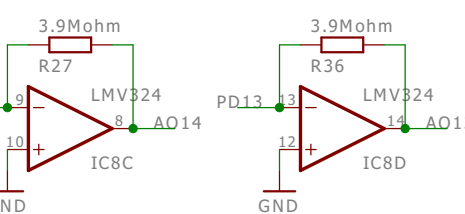
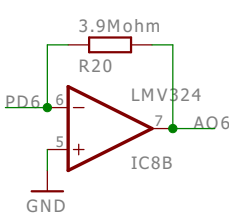
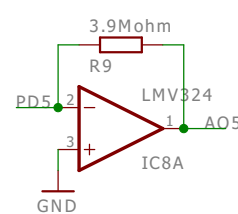
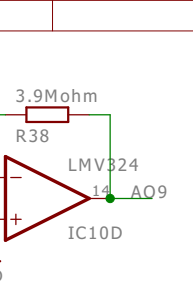
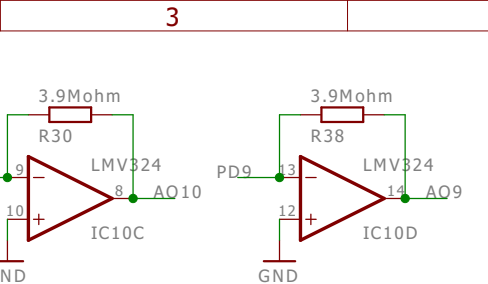
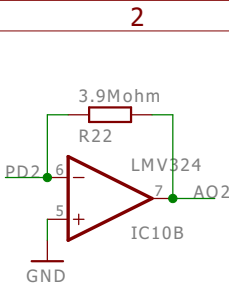
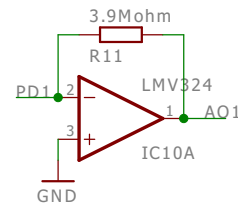
4



5



6



Copyright Miroculus 2016.

This documentation describes Open Hardware and is licensed under the CERN OHL v. 1.2.

You may redistribute and modify this documentation under the terms of the CERN OHL v.1.2. (<http://ohwr.org/cernohl>). This documentation is distributed WITHOUT ANY EXPRESS OR IMPLIED WARRANTY, INCLUDING OF MERCHANTABILITY, SATISFACTORY QUALITY AND FITNESS FOR A PARTICULAR PURPOSE. Please see the CERN OHL v.1.2 for applicable conditions

SENSOR BOARD V2
JUHO TERRIJARVI
BASED ON WORK BY
ALEJANDRO U. BOFILL
ARDUINO

AMPLIFIERS 1
sensor_002
11.4.2016 20:50
Sheet: 1/1

1

2

3

4

5

6

1

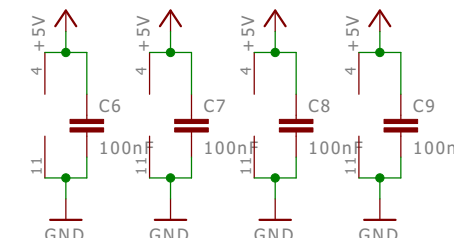
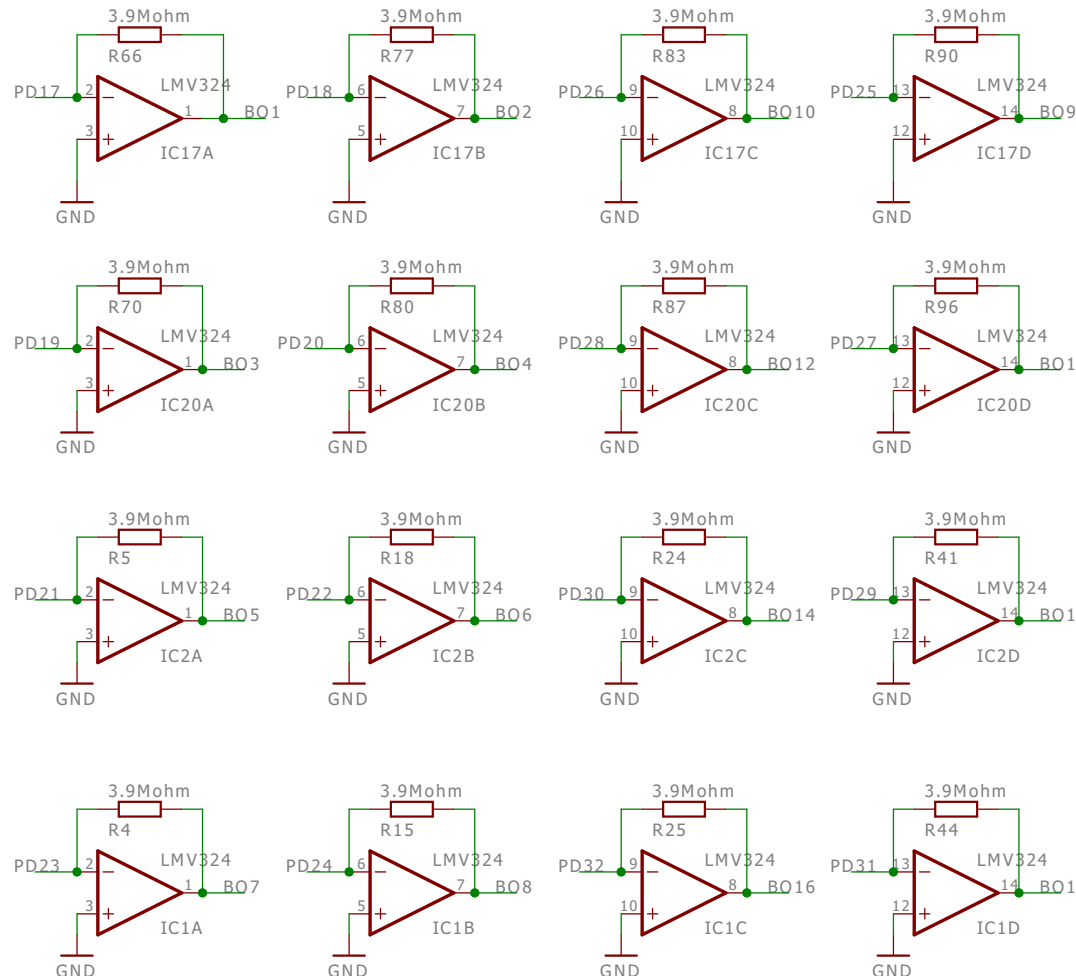
2

3

4

5

6



Copyright Miroculus 2016.

This documentation describes Open Hardware and is licensed under the CERN OHL v. 1.2.

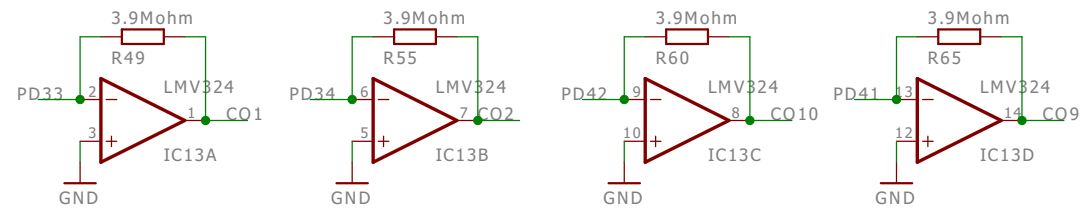
You may redistribute and modify this documentation under the terms of the CERN OHL v.1.2. (<http://ohwr.org/cernohl>). This documentation is distributed WITHOUT ANY EXPRESS OR IMPLIED WARRANTY, INCLUDING OF MERCHANTABILITY, SATISFACTORY QUALITY AND FITNESS FOR A PARTICULAR PURPOSE. Please see the CERN OHL v.1.2 for applicable conditions

SENSOR BOARD V2
JUHO TERRIJARVI
BASED ON WORK BY
ALEJANDRO V. BOFILL
ARDUINO

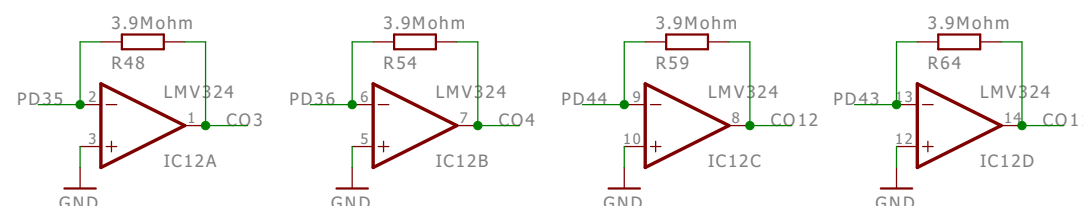
AMPLIFIERS 2
sensor_002
11.4.2016 20:50
Sheet: 1/1

1 2 3 4 5 6

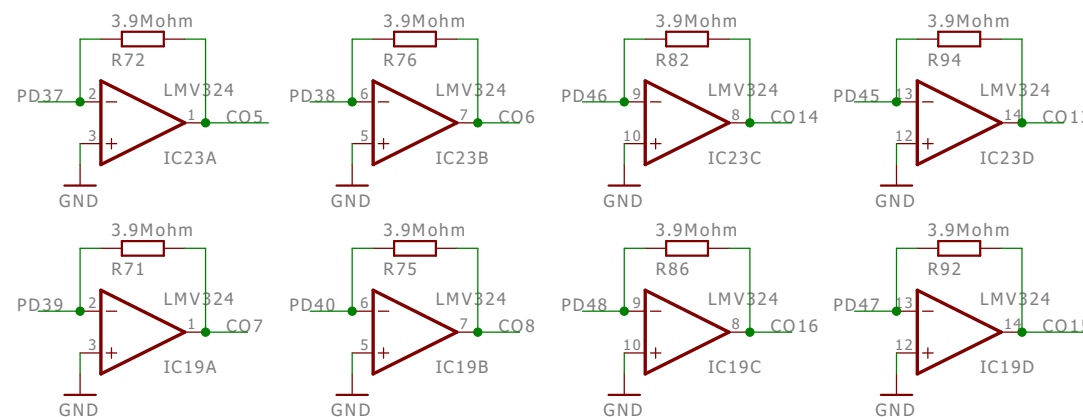
A



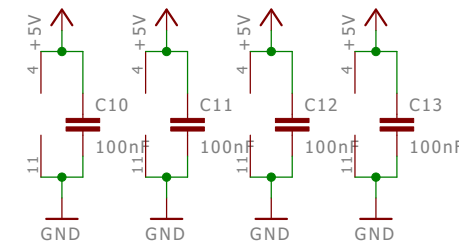
B



C



D



Copyright Miroculus 2016.

This documentation describes Open Hardware and is licensed under the CERN OHL v.1.2.

You may redistribute and modify this documentation under the terms of the CERN OHL v.1.2. (<http://ohwr.org/cernohl>). This documentation is distributed WITHOUT ANY EXPRESS OR IMPLIED WARRANTY, INCLUDING OF MERCHANTABILITY, SATISFACTORY QUALITY AND FITNESS FOR A PARTICULAR PURPOSE. Please see the CERN OHL v.1.2 for applicable conditions

SENSOR BOARD V2
JUHO TERRIJARVI
BASED ON WORK BY
ALEJANDRO V. BOFILL
ARDUINO

AMPLIFIERS 3
sensor_002
11.4.2016 20:50
Sheet: 1/1

1 2 3 4 5 6

POWER

A

MKDSN1,5/2-5,08

X1-2

X1-1

+5V

GND

- X2-10 AR0
- X2-9 AR1
- X2-8 AR2
- X2-7 AR3
- X2-6 AR4
- X2-5 AR5
- X2-4 S1
- X2-3 S0
- X2-2 S3
- MKDSN1,5/10-5,08 X2-1 S2

A

B

C

D



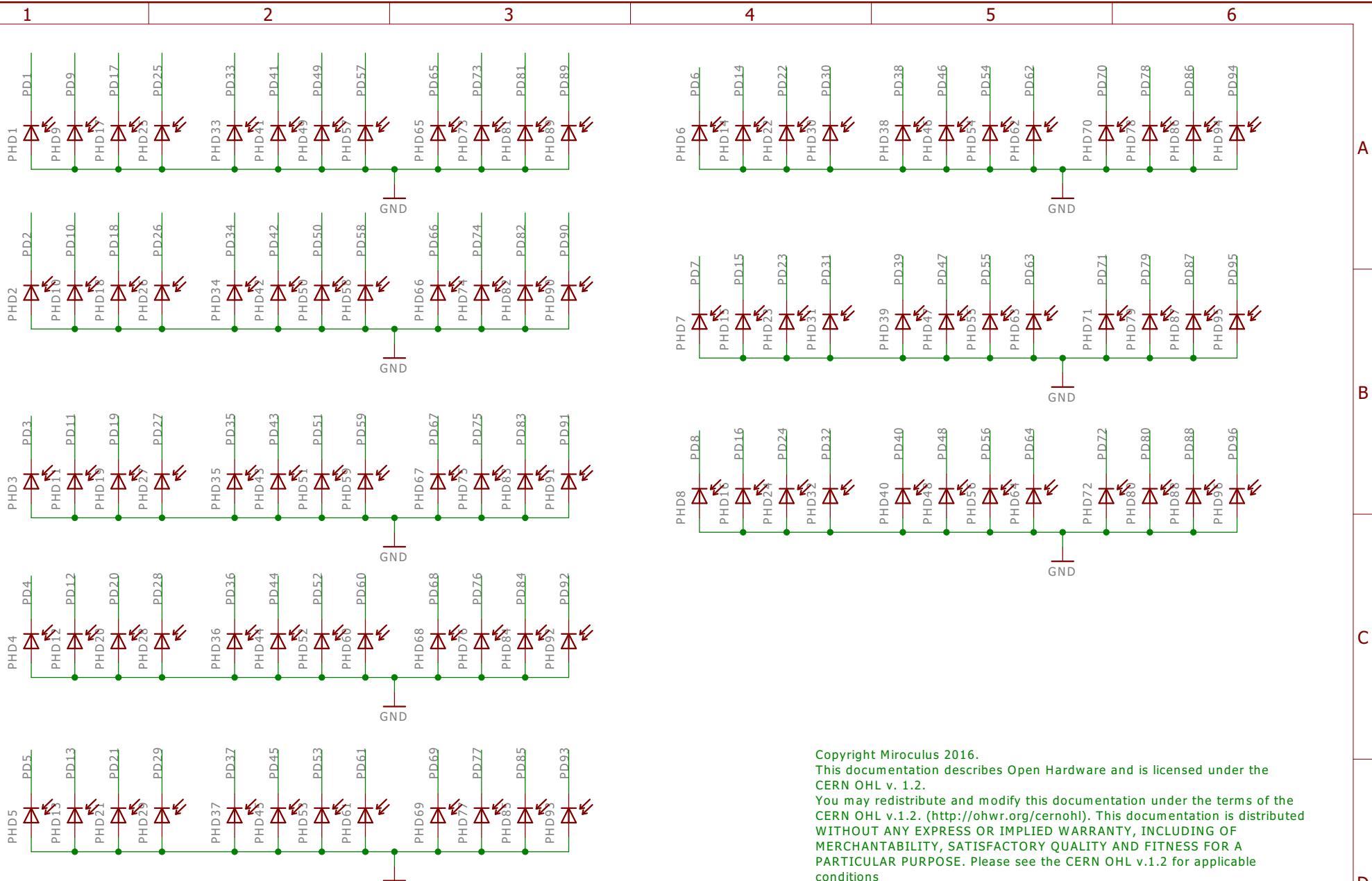
Copyright Miroculus 2016.

This documentation describes Open Hardware and is licensed under the CERN OHL v. 1.2.

You may redistribute and modify this documentation under the terms of the CERN OHL v.1.2. (<http://ohwr.org/cernohl>). This documentation is distributed WITHOUT ANY EXPRESS OR IMPLIED WARRANTY, INCLUDING OF MERCHANTABILITY, SATISFACTORY QUALITY AND FITNESS FOR A PARTICULAR PURPOSE. Please see the CERN OHL v.1.2 for applicable conditions

SENSOR BOARD U2
JUHO TERRIJARVI
BASED ON WORK BY
ALEJANDRO V. BOFILL
ARDUINO

POWER/PORTS	
sensor_002	
11.4.2016 20:50	
Sheet: 1/1	

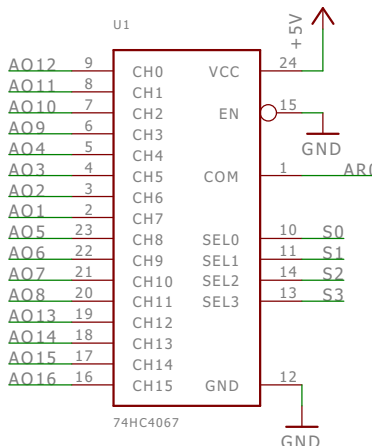


Copyright Miroculus 2016.
 This documentation describes Open Hardware and is licensed under the
 CERN OHL v. 1.2.
 You may redistribute and modify this documentation under the terms of the
 CERN OHL v.1.2. (<http://ohwr.org/cernohl>). This documentation is distributed
 WITHOUT ANY EXPRESS OR IMPLIED WARRANTY, INCLUDING OF
 MERCHANTABILITY, SATISFACTORY QUALITY AND FITNESS FOR A
 PARTICULAR PURPOSE. Please see the CERN OHL v.1.2 for applicable
 conditions

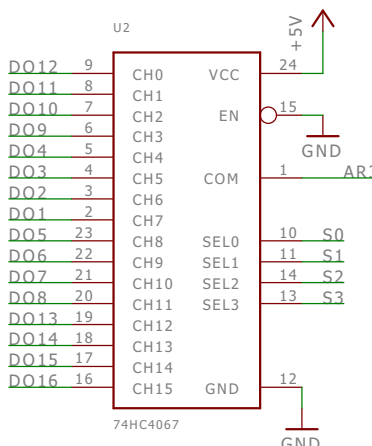
SENSOR BOARD U2
 JUHO TERRIJARVI
 BASED ON WORK BY
 ALEJANDRO V. BOFILL
 ARDUINO

PHOTODIODES
 sensor_002
 11.4.2016 20:50
 Sheet: 1/1

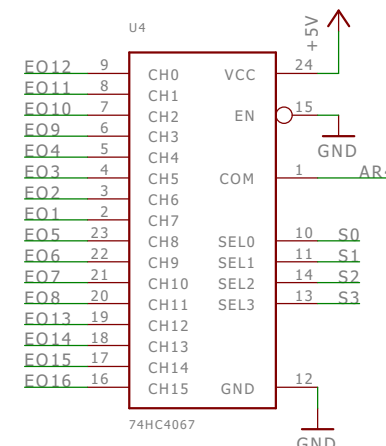
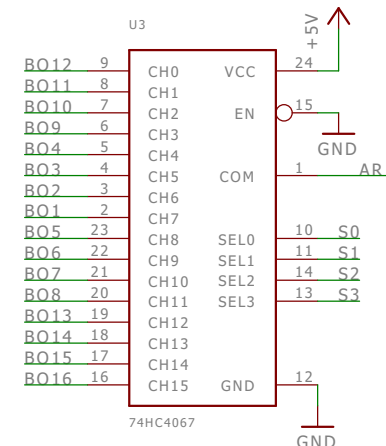
A



B



C



D

Copyright Miroculus 2016.

This documentation describes Open Hardware and is licensed under the
CERN OHL v. 1.2.

You may redistribute and modify this documentation under the terms of the
CERN OHL v.1.2. (<http://ohwr.org/cernohl>). This documentation is distributed
WITHOUT ANY EXPRESS OR IMPLIED WARRANTY, INCLUDING OF
MERCHANTABILITY, SATISFACTORY QUALITY AND FITNESS FOR A
PARTICULAR PURPOSE. Please see the CERN OHL v.1.2 for applicable
conditions

SENSOR BOARD U2
JUHO TERRIJARVI
BASED ON WORK BY
ALEJANDRO V. BOFILL
ARDUINO

MULTIPLEXORS

sensor_002

11.4.2016 20:50

Sheet: 1/1

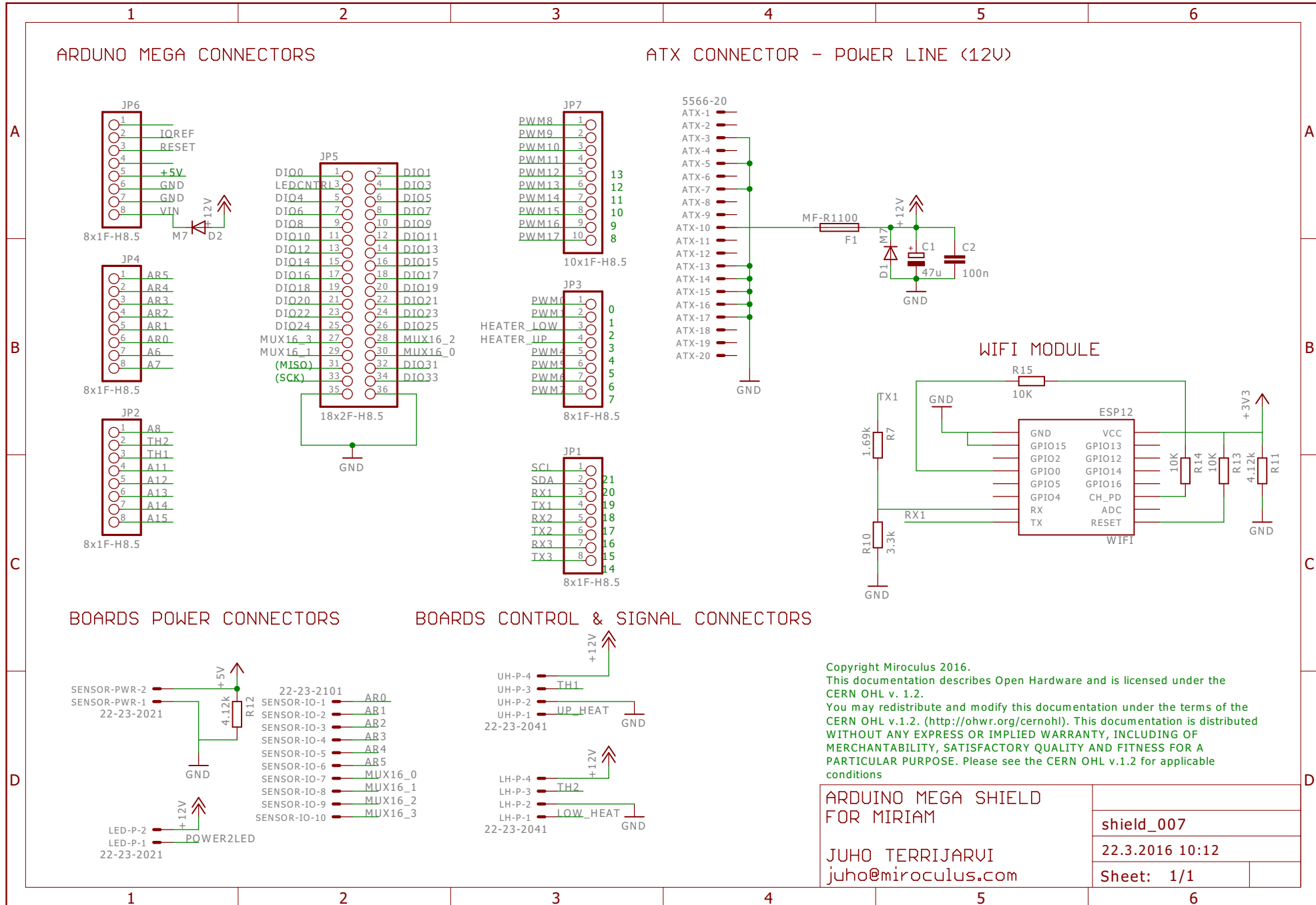
A

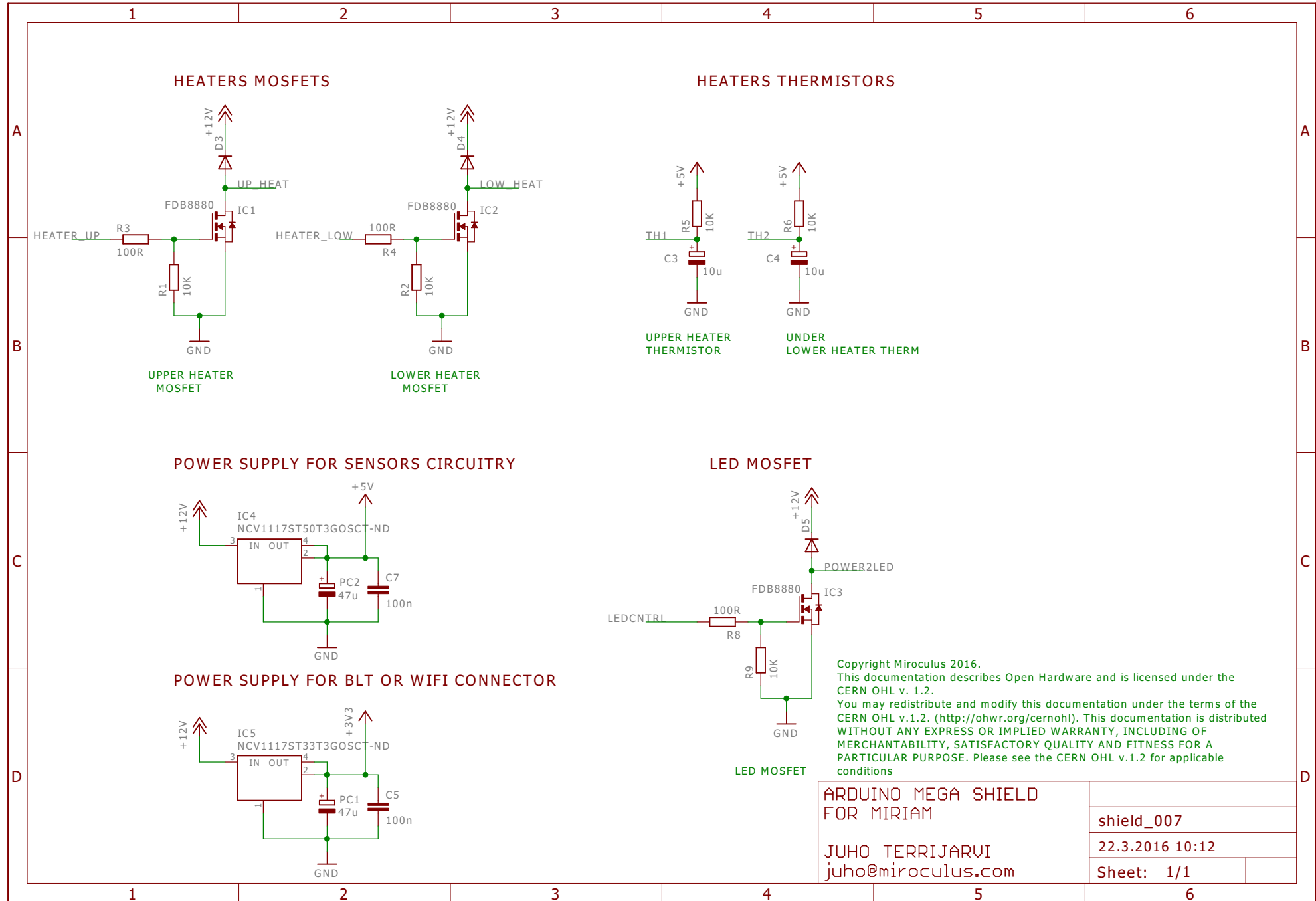
B

C

D

PCB: sensor_002					
part	pcs/pcb	Value	Package	Description	Remark
C1,C2,C3,C4,C5,C6,C7,C8,C9,C10,C11,C12,C13,C14,C15,C16,C17,C18,C19, C20,C21,C22,C23,C25	24	100nF	C0603	C-EUC0603	CAPACITOR, European symbol
R1,R2,R3,R4,R5,R7,R8,R9,R10,R11,R12,R13,R14,R15,R16,R17,R18,R19,R2 0,R21,R22,R23,R24,R25,R26,R27,R28,R29,R30,R31,R32,R33,R34,R35,R36, R37,R38,R39,R40,R41,R42,R43,R44,R45,R46,R47,R48,R49,R50,R51,R52,R5 3,R54,R55,R56,R57,R58,R59,R60,R61,R62,R63,R64,R65,R66,R67,R68,R69, R70,R71,R72,R73,R74,R75,R76,R77,R78,R79,R80,R81,R82,R83,R84,R85,R8 6,R87,R88,R89,R90,R91,R92,R93,R94,R95,R96,R97	96	3.9Mohm	R0603	R-EU_R0603	RESISTOR, European symbol
U1,U2,U3,U4,U5,U6	6	74HC4067	SSOP24	MUX-1X16	1x16 Channel Analog Multiplexer/Demultiplexer [Part No.]
PHD1,PHD2,PHD3,PHD4,PHD5,PHD6,PHD7,PHD8,PHD9,PHD10,PHD11,PH D12,PHD13,PHD14,PHD15,PHD16,PHD17,PHD18,PHD19,PHD20,PHD21,P HD22,PHD23,PHD24,PHD25,PHD26,PHD27,PHD28,PHD29,PHD30,PHD31, PHD32,PHD33,PHD34,PHD35,PHD36,PHD37,PHD38,PHD39,PHD40,PHD4 1,PHD42,PHD43,PHD44,PHD45,PHD46,PHD47,PHD48,PHD49,PHD50,PHD 51,PHD52,PHD53,PHD54,PHD55,PHD56,PHD57,PHD58,PHD59,PHD60,PH D61,PHD62,PHD63,PHD64,PHD65,PHD66,PHD67,PHD68,PHD69,PHD70,P HD71,PHD72,PHD73,PHD74,PHD75,PHD76,PHD77,PHD78,PHD79,PHD80, PHD81,PHD82,PHD83,PHD84,PHD85,PHD86,PHD87,PHD88,PHD89,PHD9 0,PHD91,PHD92,PHD93,PHD94,PHD95,PHD96	96	CLS15-22C/L213	PD_0.2	PD_0.2	Photodiode
FD1,FD2,FD3,FD4,FD5,FD6	6	FIDUCIALMOUN	FIDUCIALMOUNT	FIDUCIA-MOUNT	
IC1,IC2,IC3,IC4,IC5,IC6,IC7,IC8,IC9,IC10,IC11,IC12,IC13,IC14,IC15,IC16,IC1 7,IC18,IC19,IC20,IC21,IC22,IC23,IC24	24	LMV324	SO14		OP AMP
X2	1	MKDSN1,5/10-5	MKDSN1,5/10-5,08	MKDSN1,5/10-5,08	MKDSN 1,5/10-5,08 Printklemme
X1	1	MKDSN1,5/2-5,0	MKDSN1,5/2-5,08	MKDSN1,5/2-5,08	MKDSN 1,5/ 2-5,08 Printklemme





PCB:	SHIELD_007				
part	pcs/pcb	Value	Package	Description	Remark
R7	1	1.69k	R0603	RESISTOR, European symbol	
R3, R4, R8	3	100R	R0603	RESISTOR, European symbol	
C2, C5, C7	3	100n	C0603	CAPACITOR, European symbol	
R1, R2, R5, R6, R9, R13, R14, R15	8	10K	R0603	RESISTOR, European symbol	
C3, C4	2	10u	A/3216-18R	POLARIZED CAPACITOR, European symbol	
JP7	1	10x1F-H8.5	1X10	PIN HEADER	
JP5	1	18x2F-H8.5	2X18	PIN HEADER	
LED-P, SENSOR-PWR	2	22-23-2021	22-23-2021	.100 (2.54mm) Center Header - 2 Pin"	
LH-P, UH-P	2	22-23-2041	22-23-2041	.100 (2.54mm) Center Header - 4 Pin"	
SENSOR-IO	1	22-23-2101	22-23-2101	.100 (2.54mm) Center Header - 10 Pin"	
R10	1	3.3k	R0603	RESISTOR, European symbol	
R11, R12	2	4.12k	R0603	RESISTOR, European symbol	
C1, PC1, PC2	3	47u	PANASONIC_D	POLARIZED CAPACITOR, European symbol	
ATX	1	5566-20	5566-20	Mini FIT connector 20 pol	
JP1, JP2, JP3, JP4, JP6	5	8x1F-H8.5	1X08	PIN HEADER	
IC1, IC2, IC3	3	FDB8880	FDB8880	FDB8880 N-Channel PowerTrench MOSFET	
WIFI	1	ESP12	ESP12	ESP8266 Wifi module 12	
D1, D2	2	M7	SMB	DIODE	
F1	1	MF-R1100	LITTLEFUSE	LITTLEFUSE	
IC4	1	NCV1117ST50T3GOSCT-ND	SOT223	Adjustable Output Low Dropout Voltage Regulator 800 mA	
IC5	1	NCV1117ST33T3GOSCT-ND		Adjustable Output Low Dropout Voltage Regulator 800 mA	
D3, D4, D5	3	RGL34A	DO-213AA_DIODE	RGL34A thru RGL34K	